



Review

# Nanomaterials-Functionalized Hydrogels for the Treatment of Cutaneous Wounds

Yangkun Liu <sup>1,2</sup> , Gongmeiyue Su <sup>1,2</sup>, Ruoyao Zhang <sup>1,2</sup>, Rongji Dai <sup>2,3</sup> and Zhao Li <sup>1,2,\*</sup>

<sup>1</sup> Institute of Engineering Medicine, School of Medical Technology, Beijing Institute of Technology, 5 South Zhongguancun Street, Haidian District, Beijing 100081, China

<sup>2</sup> Beijing Key Laboratory for Separation and Analysis in Biomedicine and Pharmaceuticals, Beijing Institute of Technology, 5 South Zhongguancun Street, Haidian District, Beijing 100081, China

<sup>3</sup> School of Life Science, Beijing Institute of Technology, 5 South Zhongguancun Street, Haidian District, Beijing 100081, China

\* Correspondence: lizhao@bit.edu.cn

**Abstract:** Hydrogels have been utilized extensively in the field of cutaneous wound treatment. The introduction of nanomaterials (NMs), which are a big category of materials with diverse functionalities, can endow the hydrogels with additional and multiple functions to meet the demand for a comprehensive performance in wound dressings. Therefore, NMs-functionalized hydrogels (NMFHs) as wound dressings have drawn intensive attention recently. Herein, an overview of reports about NMFHs for the treatment of cutaneous wounds in the past five years is provided. Firstly, fabrication strategies, which are mainly divided into physical embedding and chemical synthesis of the NMFHs, are summarized and illustrated. Then, functions of the NMFHs brought by the NMs are reviewed, including hemostasis, antimicrobial activity, conductivity, regulation of reactive oxygen species (ROS) level, and stimulus responsiveness (pH responsiveness, photo-responsiveness, and magnetic responsiveness). Finally, current challenges and future perspectives in this field are discussed with the hope of inspiring additional ideas.

**Keywords:** nanomaterials; functionalization; hydrogels; treatment; cutaneous wounds



**Citation:** Liu, Y.; Su, G.; Zhang, R.; Dai, R.; Li, Z. Nanomaterials-Functionalized Hydrogels for the Treatment of Cutaneous Wounds. *Int. J. Mol. Sci.* **2023**, *24*, 336. <https://doi.org/10.3390/ijms24010336>

Academic Editor: David Mills

Received: 22 November 2022

Revised: 17 December 2022

Accepted: 21 December 2022

Published: 25 December 2022



**Copyright:** © 2022 by the authors. Licensee MDPI, Basel, Switzerland. This article is an open access article distributed under the terms and conditions of the Creative Commons Attribution (CC BY) license (<https://creativecommons.org/licenses/by/4.0/>).

## 1. Introduction

The skin is the largest organ of the body and performs secretory, excretory, and absorptive functions. It can also be used to sense touch, temperature, pain, and itches [1]. The human body will be tremendously affected by skin damage [2–4]. The imperative need for rapid clinical progress in the treatment of skin wounds is urgent, and incorrect care can lead to irreversible consequences that can have a huge impact on patients [5,6]. Human skin is capable of some self-healing, but the long-term repair process inevitably accompanies chronic wound infections, which in turn impede the healing process [7]. Therefore, it is necessary to develop effective in vitro tissue engineering materials to promote rapid skin wound healing [8]. Ideal wound dressings need to be biocompatible, adhere to the wound tightly, stop the bleeding for several hours, provide a suitable environment for healing, be antimicrobial, create a barrier from the outside environment, and be easily applied [9–11]. Currently, numerous forms of dressings have been developed to accelerate skin wound healing, such as scaffolds [12–14], electrospinning nanofibers mats [15–17], sponges [18–20], and hydrogels [21–23]. Indeed, hydrogels have drawn great attention in recent years [24,25].

Hydrogels are crosslinked 3D networks that swell with large amounts of water [26,27]. They have been widely used in dressings because they can keep the wound moist, cool the wound, absorb inflammatory exudates from the wound, provide a breathable microenvironment, prevent anaerobic bacteria from colonizing, and release preloaded therapeutic agents [28–31]. However, the biological efficiency of biomaterials is typically insufficient

for multifunctional applications when they are created as hydrogel matrix alone. Thus, a common way to improve the comprehensive performance of hydrogels as wound dressings is to introduce modifiers for targeted functionalization.

Nanomaterials (NMs) are tiny particles, ranging in size from 1 to 100 nm [30,32]. They have been widely used in various fields, such as catheter coatings, antimicrobial agents, and biomarker detection [33–35]. Additionally, they play irreplaceable roles in hydrogels used for cutaneous wound treatment, even outperforming the biological efficacy of drugs in some aspects. A nanometer-level scale can endow the materials with various superiorities: (1) NMs can generate new or enhanced electricity, light, heat, and magnetism; (2) they have stronger penetrating power to destroy structures of bacteria and viruses than conventional wound healing drugs or materials with larger scales; (3) they can change the pharmacokinetics and drug delivery efficiency; (4) the shape-tunable properties of NMs and the specific surface area can provide more binding sites for the attachment of bioactive substances such as drugs, nucleic acids, and proteins [36–40]. Recently, a variety of NM-loaded hydrogels with diverse functionalities have been developed as advanced wound dressings. The hydrogel can be endowed with the inherent properties of NMs. For NMs, hydrogels can offer a stable environment. Moreover, they can also avoid the explosive release and accumulation of NMs in wounds, which may result in biotoxicity [41]. The combination of NMs and hydrogels provides more opportunities for the treatment of skin wounds. Therefore, a systemic summary of this field will benefit its development.

Herein, the progress of NMs-functionalized hydrogels (NMFHs) in cutaneous wound treatment over the past five years is reviewed. Firstly, the fabrication strategies of the NMFHs are summarized and illustrated. Then, functions brought by NMs to the NMFHs are overviewed. Furthermore, the current research challenges and prospects of this field are also discussed.

## 2. Fabrication Strategies

Based on the mode of introduction of NMs into hydrogel networks, fabrication strategies for NMFHs can be mainly divided into two categories, which are physical embedding and chemical synthesis (Figure 1). For the former, no covalent bonds exist between NMs and gel network chains. For the latter, NMs form covalent bonds with gel networks. These NMs usually play the role of crosslinking points. In addition, some NMs with a specific state, such as nanowires, can also play the role of chains to form the network through covalently linking by linkers.

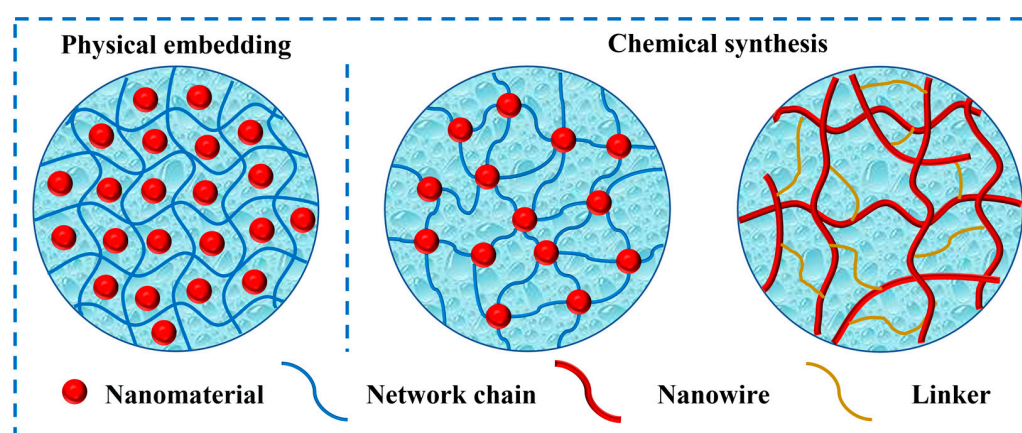


**Figure 1.** Schematic of fabrication strategies of physical embedding and chemical synthesis of NMFHs.

### 2.1. Physical Embedding

Physical embedding is the most common and convenient strategy to fabricate NMFHs. For example, Xu and Chen et al. constructed an antimicrobial hydrogel dressing via loading

Ag nanoparticles (NPs) into a poly(vinyl alcohol) (PVA)/sodium alginate (SA)/carboxymethyl chitosan (CMCS) (PVA/SA/CMCS)-based network [42]. As reducing agents, hydroxyl and carboxyl groups on sodium alginate (Alg) chelated  $\text{Ag}^+$  which was reduced to  $\text{Ag}^0$  to form the Ag NPs-embedded matrix (Figure 2A). NMs can also form non-covalent interactions with gel network chains, such as electrostatic interaction and hydrogen bonds. Xia et al. designed a nanocomposite hydrogel based on Alg and edaravone-loaded Eudragit NPs (EDA NPs). Eudragit NPs were positively charged polymeric NMs, which could bind to negatively charged Alg chains through electrostatic interactions to form the hydrogel [43]. Keleher et al. prepared an antimicrobial hydrogel dressing by introducing Ag-coated  $\text{TiO}_2$  NPs (Ag/ $\text{TiO}_2$  NPs) into an SA-based matrix [44]. Due to the existence of many hydroxyl groups on the NPs core ( $\text{TiO}_2$ ), hydrogen bonds formed between the NPs and alginate chains. This non-covalent interaction results in a higher packing density (Figure 2B).

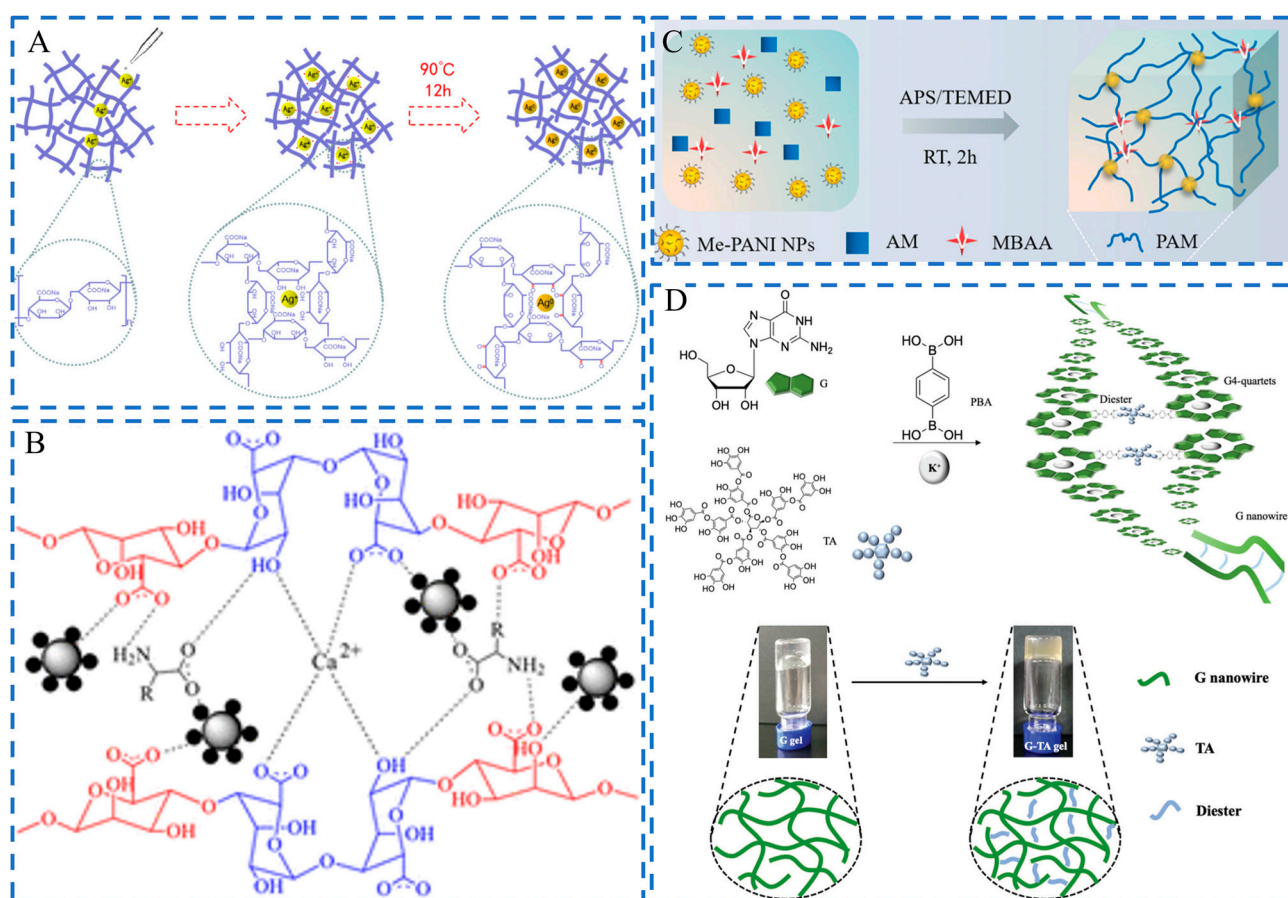


**Figure 2.** Schematics of fabrications of NMFHs by physical embedding and chemical synthesis. (A) Formation of an NMFH through embedding Ag NPs in the PVA/SA/CMCS-based network. Adapted with permission [42]. Copyright 2020, Elsevier. (B) The network structure of the NMFH is based on SA, Ag@TiO<sub>2</sub> NPs, amino acids, and Ca<sup>2+</sup>. Adapted with permission [44]. Copyright 2020, The American Chemical Society. (C) Schematic of the formation of the NMFH from Me-PANI NPs, AM, and *N,N'*-methylenebisacrylamide (MBAA) through free radical copolymerization. Adapted with permission [45]. Copyright 2021, Wiley-VCH. (D) Schematic of the formation of the NMFH based on G NWs, K<sup>+</sup>, TA, and PBA. Adapted with permission [46]. Copyright 2022, The Royal Society of Chemistry.

## 2.2. Chemical Synthesis

The NMs bonded to gel networks by covalent bonds are usually more stable than the physically embedded ones. The strategy of chemical synthesis has been applied to the fabrication of NMFHs through the introduction of organic NPs or functionalized inorganic

NPs into gel networks. For example, Pang and Zhu developed a photothermal antibacterial hydrogel through introducing double bond-ended polyaniline NPs (Me-PANI NPs) into the polyacrylamide (PAM) network [45]. The Me-PANI NPs were self-assembled from the amphiphilic copolymer PANI-g-Methacrylated glycol chitosan (MeCC) which was formed via grafting the hydrophobic PANI onto the hydrophilic MeGC chain. The NPs acted as the crosslinking points to form the hydrogel through free radical copolymerization among double bonds on the NPs and acrylamide (AM) (Figure 2C). NMs with specific states can also act as network chains to form hydrogels through covalent linking by linkers. This is a kind of special chemical synthesis approach. Zhao and Chen et al. fabricated a hydrogel based on guanosine nanowires (G NWs), tannic acid (TA), 1,4-phenylenediboric acid (PBA), and  $K^+$  through a one-pot method [46]. G NWs were first created through the hierarchical assembly of guanosine and  $K^+$ . Then the hydrogel was fabricated from G NWs, TA, and PBA through the formation of borate esters between hydroxyl groups on G NWs, TA, and boronic acid groups on PBA (Figure 2D).

### 3. Functions

In this section, NMFHs in cutaneous wound treatment are overviewed from the perspective of the function NMs bring to the hydrogels. Five categories of functions which are hemostasis, antimicrobial activity, conductivity, regulation of reactive oxygen species (ROS) level, and stimulus responsiveness (pH responsiveness, photo-to-responsiveness, and magnetic responsiveness) are involved (Figure 3).

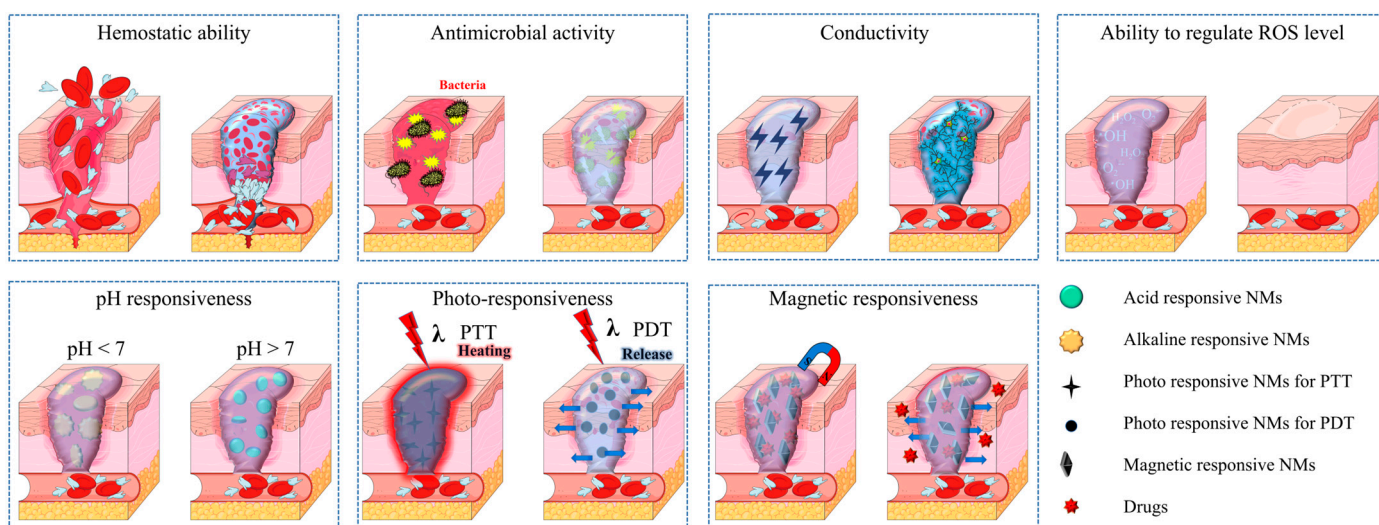


**Figure 3.** Schematic of functions of NMFHs for the cutaneous wound treatment. (PTT: photothermal therapy; PDT: photodynamic therapy).

#### 3.1. Hemostatic Ability

The primary therapeutic treatment method for penetrating wounds is hemostasis, which acts in the initial phase of the wound. A critical aspect of healing cutaneous wounds is maintaining hemostasis. [47–49]. Patients suffering from penetrating wounds require rapid hemostatic treatment in order to avoid serious complications, such as amputation and death [50]. The process of hemostasis consists of three synergistically ordered processes: vasospasm and hemostasis, the formation of platelet embolism, and the coagulation cascade [51]. The ideal hemostatic materials should be able to adhere to tissues quickly, be removed at the wound site, and keep long-term stability. Additionally, hemostatic hydrogels should also have strong mechanical strength to resist blood pressure [51,52].

Li et al. developed a keratin-catechin nanocomposite modified cellulose hydrogel, as presented in Figure 4A. The catechin crosslinked the keratin and then clustered into nanoparticles (NPs), which were embedded in a cellulose-based hydrogel for the treatment

of a full-thickness skin defect. The catechin endowed the hydrogel with strong adhesiveness [53], while keratin had hemostatic potential by accelerating thrombin activation and inducing platelet aggregation. They synergistically achieved rapid hemostasis [54]. Non-metallic minerals with excellent biological performances have also been used in the development of hemostatic hydrogels. Halloysite nanotubes (HNTs) are natural clays with good hemostatic and cell proliferation promotion abilities. Lu and Zhang et al. introduced them into a chitosan (CS)/oxidized dextran (ODEX)-based hydrogel to reduce hemostatic time and blood loss (Figure 4B). This hydrogel was formed by in situ crosslinking through the Schiff base reaction between amino groups ( $-NH_2$ ) in CS and aldehyde groups ( $-CHO$ ) in ODEX. Besides, the composite pre gel solution could transfer to hydrogel within 1 s after injection, which could adapt to wounds with different shapes [55]. Cuttlefish melanin is a natural biomaterial with a catechol structure. It can significantly improve the adhesion performance of hydrogels, which is a crucial property that hemostatic materials ought to have [56,57]. Guo et al. developed a composite hydrogel based on adipic dihydrazide-modified hyaluronic acid (HA), benzaldehyde-functionalized poly(ethylene glycol)-*co*-poly(glycerol sebacate) (PEGSB), and cuttlefish melanin NPs [58]. This hydrogel exhibited great adhesive and hemostatic abilities, indicating potential for motion wound treatment in clinics.

In addition to non-metallic NPs, certain metallic NPs and their composites have been used in the development of hemostatic hydrogels. Lan et al. introduced Ag NPs into a CS/gelatin/sodium hyaluronate (SH)-based hydrogel to prepare a composite hydrogel that could control hemorrhage and promote wound healing after hemostasis surgery [59]. Ag NPs could achieve rapid hemostasis by promoting phosphatidylserine exposure, thrombin formation, and inducing platelet aggregation by activating positively charged surfaces [60,61]. Lee et al. mixed Ag@metal organic framework (Ag@MOF) with graphene oxide (GO) and loaded them into silk glue/CS-based hydrogels to affect red blood cells and platelets, accelerating thrombus formation, thus improving coagulation [62]. Xiao, Feng, Mi, and Liu et al. synthesized hydrazide-grafted HA (HAh) and aldehyde and quaternary ammonium-grafted HA (HAaq) to apply them in a permeable HA@MnO<sub>2</sub>/fibroblast growth factor 2 (FGF-2)/exosomes (Exos) hydrogel fabrication with rapid hemostatic function (Figure 4C). The positively charged quaternary ammonium group on the hydrogel could attract blood cells by the electrostatic interaction and improve the coagulation ability, while MnO<sub>2</sub>- $\epsilon$ -polylysine ( $\epsilon$ -PLys) nanosheets (NSs) in the hydrogel network could catalyze the conversion of excessive hydrogen peroxide (H<sub>2</sub>O<sub>2</sub>) generated at the wound to O<sub>2</sub>, thus removing ROS and providing O<sub>2</sub> for wound healing [63]. Jayakumar et al. developed a composite nano bio glass that was loaded into a CS hydrogel to further enhance its coagulation function. The silica, calcium, and phosphate in nano bioglass synergized with CS to achieve rapid bleeding control by activating coagulation factor XII and the intrinsic and exogenous pathways [64].

### 3.2. Antimicrobial Activity

Inhibition of bacterial infections is a primary factor in skin wound care. There is an urgent need to develop advanced materials with antimicrobial activity [65,66]. Some biopolymers used to prepare hydrogels to have inherent antimicrobial properties, such as CS [67], chitin [68], Alg [69], and bacterial cellulose [70]. The antimicrobial mechanism of these biomaterials could contribute to the destruction of the surface structure of the bacteria by the biological materials, resulting in the outflow of the fluid in the cells or the coating of the bacteria, resulting in cell death [71,72]. In addition, some PEG-based hydrogels [73], cationic peptide-based hydrogels [74], and zwitterionic hydrogels [75] have antifouling properties and can promote antimicrobial activity by inhibiting bacterial adhesion. However, the antibacterial activity of the above hydrogels is limited, and the antifouling hydrogels only act as a barrier against unfriendly factors. It is necessary to introduce ingredients with antibacterial activity. Many studies have introduced antibiotics to improve the antibacterial activity of hydrogels, such as tetracycline [76], gentamicin [77],

amoxicillin [78], and ciprofloxacin [79]. Although antibiotics have been widely used in clinical treatment, the increasing severity of drug resistance should not be ignored. Therefore, it is meaningful to develop new antibacterial strategies [2]. NMs are considered to be effective alternatives to antibiotics and there are many reports about the introduction of NMs as antibacterial agents or antibacterial enhancers into hydrogels.

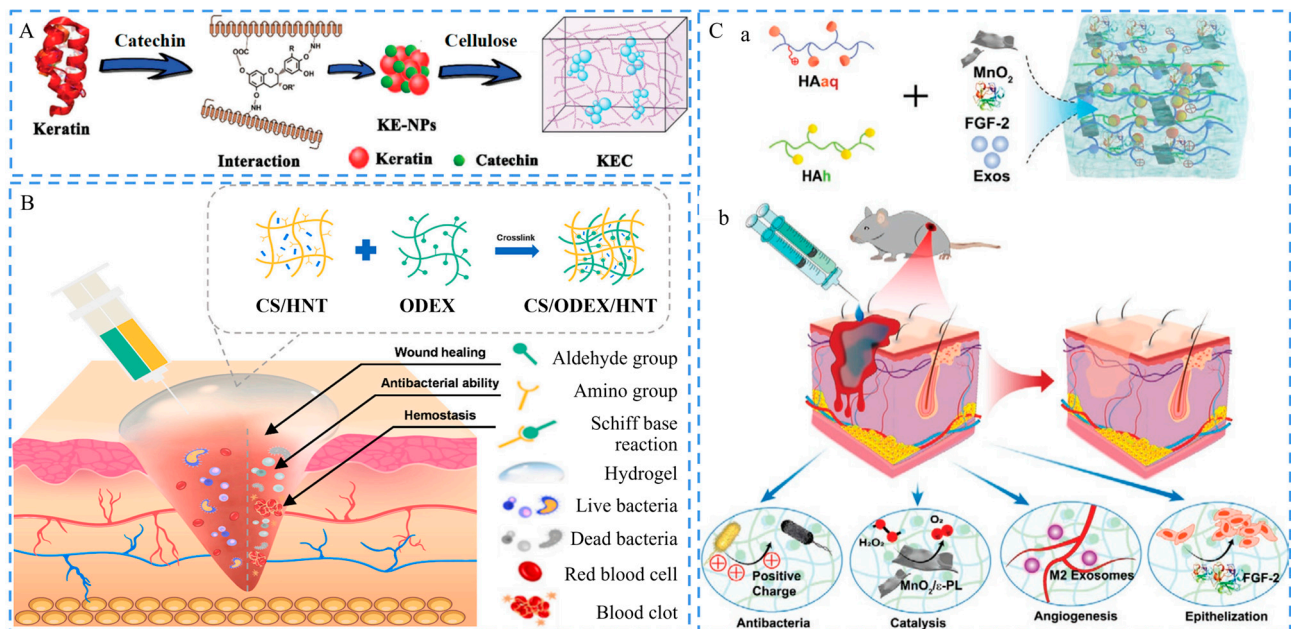


**Figure 4.** Schematics of hemostatic hydrogels. (A) Schematic of molecular assembly of keratin-catechin (KE)-NPs and formation of the cellulose/keratin-catechin composite hydrogel (KEC). Reproduced with permission [54]. Copyright 2018, Royal Society of Chemistry. (B) Schematic of the CS/ODEX/HNT hydrogel. The hydrogel was prepared in situ by the crosslinking between CS and ODEX via the Schiff base reaction and showed homeostatic and antibacterial abilities. Reproduced with permission [55]. Copyright 2021, Elsevier. (C) Preparation and application of the HA@MnO<sub>2</sub>/FGF-2/Exos hydrogel. (a) The preparation procedure for the hydrogel. (b) The hydrogel could promote wound healing by killing bacteria, catalyzing H<sub>2</sub>O<sub>2</sub> decomposition, and accelerating neovascularization and re-epithelialization. Adapted with permission [63]. Copyright 2021, Wiley-VCH.

For instance, Ag NPs are the most widely used metal NMs in the antibacterial materials development because they can effectively resist almost all types of infections [80]. The antibacterial mechanism of Ag NPs is evident. (1) They can directly adhere to the cell wall and cell membrane, causing obvious morphological changes. (2) The neutralization between Ag NPs and bacterial surfaces changes the cell-membrane permeability, resulting in bacterial death. (3) Ag NPs can bind to cell membrane proteins and intracellular components (lipids, proteins, and DNA), which could also affect transcription, translation, and glucose metabolism. (4) Ag NPs produced by oxidative solubilization can block the transport and release of K<sup>+</sup> and prevent the synthesis of adenosine triphosphate [81–84].

Ren et al. added Ag NPs into a CS/konjac glucomannan hydrogel to obtain the NMFH that showed great prospects as a safe wound dressing [85]. This hydrogel matrix acted as a carrier to avoid the burst release of Ag NPs and reduce their cytotoxicity, achieving continuous release to inhibit the inflammatory response. In addition, it was reported that the doping of TiO<sub>2</sub> with a small amount of Ag could improve not only the antibacterial activity, but also the mechanical properties [86,87]. As an example, Ag-doped TiO<sub>2</sub> (Ag/TiO<sub>2</sub>) NPs were synthesized by a chemical reduction process and then dispersed in a poly(vinyl alcohol) (PVA) matrix to obtain a hydrogel through a repeated freeze-thawing process. This hydrogel exhibited good antimicrobial activity due to the

light-induced ROS and significantly accelerated wound healing [88]. Zhang and Wu et al. utilized Ag NPs as an antibacterial enhancer, introducing them into a matrix based on cationic chitosan and anionic dextran to develop an antifouling hydrogel [89]. The ratio of the two polymers was optimized to achieve a near zero potential for the hydrogel, thus endowing it with an antifouling property. In addition, the introduction of Ag NPs endowed the hydrogel with continuous and broad-spectrum antibacterial activity. Furthermore, Ag oxides have also been proven to have antibacterial activity. Mohammadimehr et al. loaded Ag<sub>2</sub>O/SiO<sub>2</sub> and calendula officinalis flower extract in a CS/sodium alginate (SA)/PVA hydrogel, which showed great antibacterial activity and potential to promote wound healing [90]. Besides, various types of composite hydrogels employing Ag NPs in synergy with other types of NMs as antimicrobial components have been reported, such as Ag NPs combined with g-C<sub>3</sub>N<sub>4</sub>/TiO<sub>2</sub> [91], melatonin [92], and GO [86].

Except for Ag NMs, other metal NMs also showed good antimicrobial activities against lethal viruses and microorganisms [93]. Numerous studies have demonstrated that ZnO has high antimicrobial activity and that it can be applied to cutaneous wound treatment [94]. Zhao et al. added ZnO NPs to a sodium alginate-chitosan oligosaccharide (SA-COS-ZnO) hydrogel [95] (Figure 5A). The isoelectric point of ZnO NPs is 9–10, and H<sup>+</sup> from the environment would transfer to the surface of ZnO NPs under physiological pH conditions, resulting in a positively charged surface (ZnOH<sup>2+</sup>) and the dissolution of Zn<sup>2+</sup>. Trace Zn could promote the formation of neovascularization, and Zn<sup>2+</sup> had antibacterial activity, which led to tissue healing and recovery. Additionally, some other common metal-based materials can also be utilized for the development of antimicrobial materials, such as Au, Cu, and Fe [96]. Zhang et al. prepared a hydrogel with excellent antibacterial ability by loading Au NPs into a heparin/PVA matrix. This hydrogel-based dressing exhibited strong antibacterial activity against Gram-positive (G<sup>+</sup>) and Gram-negative (G<sup>−</sup>) bacteria due to the introduction of Au NPs [97]. Zare and Makvandi et al. constructed a hydrogel by incorporating CuO into a sodium carboxymethylated starch network via a solution-casting technique [98]. CuO NPs were proved to have antioxidant activity because of the hydroxyl groups present on their surfaces, thus being used for the relief of oxidative stress at a wound site. The antibacterial activity of the CuO NPs was attributed to ROS generation by the released metal ions, which caused malfunction of the bacteria cell membranes. Moreover, CuO in the hydrogel exhibited excellent antibacterial and antioxidant activities, which effectively promoted wound healing. Ren and Tang et al. co-embedded glucose oxidase (GOx) with Fe<sub>3</sub>O<sub>4</sub>/TiO<sub>2</sub>/Ag<sub>3</sub>PO<sub>4</sub> nanocomplexes in a poly(acrylic acid) (PAAc)-calcium phosphate hydrogel by in situ biomimetic mineralization. This complex system functioned as a controllable ROS generator and demonstrated extraordinary antimicrobial activity in both in vitro and in vivo studies [99].

Furthermore, some non-metallic NMs also exhibit remarkable antimicrobial properties. Quercetin NPs (Qu NPs) are natural flavonoids with prominent anti-inflammatory effects that can react with polyhydroxy polymers via unreacted neighboring diols [100]. Wang et al. selected PVA as the hydrogel matrix to develop a Qu NPs-containing composite hydrogel, which exhibited excellent antimicrobial and antioxidant activities. The obtained hydrogel film could significantly promote full thickness wound healing [101]. Furthermore, carbon-based materials are also the choice of many researchers for the construction of antibacterial hydrogel dressings. Fan et al. constructed a wound dressing by co-embedding PEG-grafted hollow carbon NPs (PEG-HCNPs) and aloe rhodopsin (AE) in a poly(2-dimethylaminoethyl methacrylate)-based hydrogel [102]. This hydrogel could maintain long-term antimicrobial activity in combination with a photothermal effect (Figure 5B). Pamuła and Reczyńska-Kolman et al. prepared lipid NPs enriched with nisin and introduced them into a hydrogel based on gellan gum and Alg. The hydrogel ensured an extended release of the active ingredients, thus improving the antimicrobial activity [103]. Lin, Qu, and Liu et al. designed an NMFH based on reduced PDA NPs (rPDA NPs) and PEG [73]. The hydrogels were formed through crosslinking among rPDA NPs, 4-arm-PEG-succinimidyl carboxymethyl ester (4-arm-PEG-SCM), and 4-arm-PEG-NH<sub>2</sub> through an amide reaction. The pre gel

solution could solidify quickly within 1 s to form a barrier to achieve antifouling. Moreover, due to the photothermal effect of rPDA NPs, the hydrogel was able to realize effective bacterial eradication under the irradiation of near-infrared light (NIR).

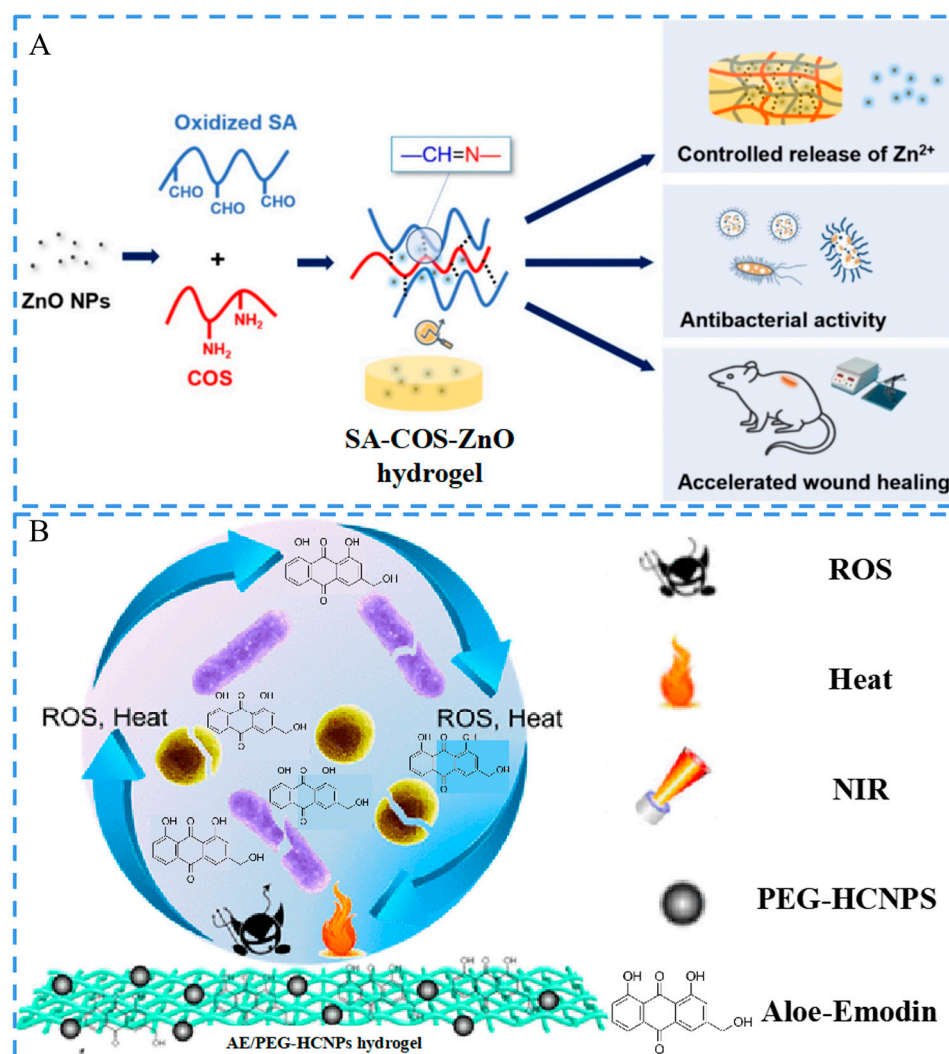


**Figure 5.** Schematics of the antimicrobial hydrogels. (A) Schematic of the construction of SA-COS-ZnO hydrogel with controlled release of Zn<sup>2+</sup>, antibacterial activity, and accelerated wound healing. Reproduced with permission [95]. Copyright 2021, Elsevier. (B) Schematic of the function of the AE/PEG-HCNPs hydrogel. The hydrogel exhibited a photothermal effect with ROS scavenging ability. The AE showed antimicrobial activity against G<sup>+</sup> and G<sup>-</sup> bacterial. Reproduced with permission [102]. Copyright 2018, The American Chemical Society.

### 3.3. Conductivity

Skin is sensitive to electrical stimulation (ES). The electrical signal plays an important role in maintaining tissue function and the regeneration [104]. Therefore, conductive hydrogels with optimal electrical transmission properties and the ability to interact with tissues are advantageous for soft tissue regeneration. Since the 1990s, researchers have been exploring the application of ES therapy to treat skin wounds [105–107]. It was demonstrated that the introduction of an external direct current electric field could accelerate the recovery of skin structure and function and regulate the migration and proliferation of cells by activating ion channels and downstream transduction signals [108,109]. In addition, the ES can also promote neovascularization and modulate the inflammatory response [110]. As a result, conductive hydrogels are in the spotlight in cutaneous wound treatment [111], in

which the NMs that have been employed for the development of conductive hydrogels can be grouped into three categories: carbon-based materials, metals, and conductive polymers.

Carbon nanotubes (CNTs) are suitable carbon-based conductive materials because they have a larger specific surface area and higher conductive efficiency than conventional conductive materials [112]. For instance, a composite conductive hydrogel for wound healing was constructed by introducing conductive complexes and carboxylate multiwalled carbon nanotubes (MWCNTs) in the gel matrix. In addition, the hydrogel also had the ability to monitor the movement of the wound, such as the change in charge of conductive material caused by the change of stress in joints or elbows [113]. Guo and his team have developed a series of conductive hydrogels based on carbon-based materials for various wounds treatment, including DA-gelatin/CS/PDA@CNTs composite hydrogel utilized for treatment of infected wound [37], *N*-carboxyethyl CS/benzaldehyde-terminated PF127/CNTs composite hydrogel used for treatment of infected full-thickness skin wound [114], and quaternized CS-graft-cyclodextrin/quaternized CS-graft-adamantane/GO-graft-cyclodextrin composite hydrogel applied for treatment of skin defects [115]. Additionally, nerve damage frequently occurs in conjunction with cutaneous wounds. Electrical signals have been found to effectively stimulate nerve repair by inducing mesenchymal stem cells to differentiate into neural cells [116,117]. Peng et al. constructed a self-powered smart patch via coating of GelMA@rGO hydrogel onto polyvinylidene fluoride (PVDF) film [118]. The PVDF film acted as a flexible piezoelectric generator for electrical stimulation, while the hydrogel served as the reservoir of chemokine and neural directing exosomes as well as the electrode to transfer electric cues. The patch could promote nerve regeneration and sensation restoration at the wound site within 23 days, exhibiting great potential in nerve-damaged wound treatment (Figure 6A).

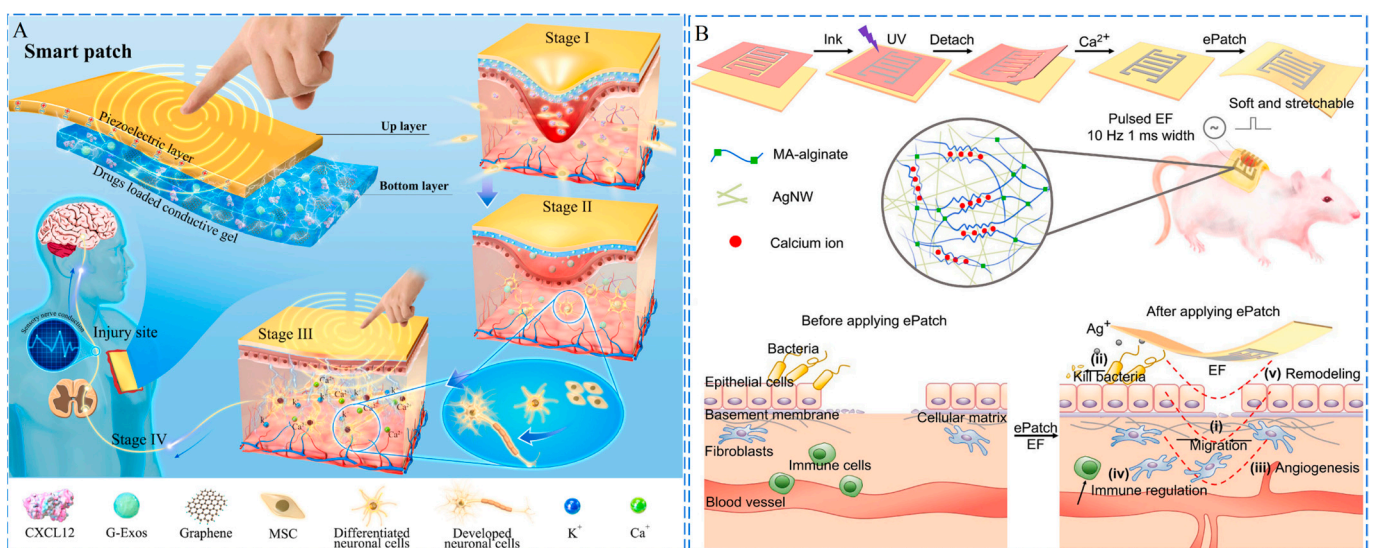


**Figure 6.** Schematics of the conductive hydrogels. (A) Schematics of the hierarchical architecture of the smart patch and its stimulation in endogenous stem cells based neural restoration and sensory function recovery. Adapted with permission [118]. Copyright 2022, Elsevier. (B) Schematics of the fabrication of ePatch and five biological activities of the ePatch during the healing process after being applied to wounded SD rats. Adapted with permission [119]. Copyright 2022, Elsevier.

Conductive hydrogels create conditions for the introduction of exogenous currents. The current parameters of the conductive layer are adjustable in the application. Ag-based NMs are good candidates for the development of conductive hydrogels. Khademhosseini et al. used Ag nanowires (NWs) as the conductive substance and methylarsonic acid (MAA) as the binder to prepare a conductive ink [119]. Figure 6B illustrates that this ink was then cast and shaped in a mold to form a conductive hydrogel patch via photocrosslinking, which achieved rapid wound healing after the addition of Pulse Width Modulation. Chen

and Zhou et al. considered Ag NPs as the conductive material and used lignin as the matrix to prepare a composite hydrogel. The lignin could reduce  $\text{Ag}^+$  in situ based on its natural reducing ability. Furthermore, the hydrogel could form a quinone/catechol structure with a dynamic redox environment, and lignin could be modified with hydroxypropyl cellulose and phenylboronic acid by a dynamic borate bond. This hydrogel is able to accelerate epithelial tissue regeneration and neovascularization, reduce inflammatory cell infiltration, promote collagen (COL) deposition, and promote  $\text{M}_2$  macrophage polarization [120]. Moreover, Zhou and Zhang et al. prepared a composite hydrogel through loading  $\text{Ti}_3\text{C}_2\text{T}_x$  MXene@PDA NSs in an oxidized HA/poly(glycerol-ethylenimine) (PGE) hydrogel matrix [121]. The nanocomposites endowed the hydrogel with excellent conductivity, improving the quality of wound healing and skin regeneration by constructing a cellular communication network through increased electrical transmission. In addition, this hydrogel also showed great adhesive properties and antimicrobial activity, which synergized with electrical conductivity to promote the healing of infected wounds and the remodeling of their appendages.

Recently, conductive polymers such as polypyrrole (Ppy) and PANI have also been increasingly used to fabricate hydrogel-based dressings. Yu and Zhou et al. prepared an oxidized chondroitin sulfate modified Ppy NPs/GelMA hydrogel with conductive ability. The hydrogel could upregulate the phosphorylation expression of the PI3K/AKT and MEK/ERK pathways by increasing the intracellular  $\text{Ca}^{2+}$  concentration. Besides, this hydrogel could also promote the migration and axon growth of PC12 neuronal cells at the cellular level and promote the regeneration of the neurovasculature and COL deposition in diabetic wound [122]. Zhang, Tao and Zhu et al. developed an E-skin patch with PF127 serving as the hydrogel matrix, and Ppy serving as the conducting medium [123]. The Ppy provided excellent photothermal and charge transport capabilities for the hydrogel due to its inherent non-radiative relaxation and conjugated structure [124,125]. The hydrogel could promote angiogenesis, COL deposition, and re-epithelialization in combination with PTT and real-time ES effectively. Moreover, Zhang et al. developed a PAAc-sulfonated HA-PANI conductive hydrogel with ES, which exhibited a powerful killing effect on G+ bacteria through specific binding to bacterial lipid calcium phosphate [126]. Unlike the macromolecular form of aniline polymorph, Guo et al. selected the oligomeric form of aniline (aniline tetramer) as the conductive matrix and synergized with oxidized HA and N-carboxyethyl CS to construct an injectable conductive hydrogel [127]. The pre gel solution could gelate rapidly under physiological conditions. Additionally, the hydrogel was also modified with amoxicillin to improve its antibacterial activity.

### 3.4. Regulation of ROS Level

ROS are a class of highly reactive chemicals derived from molecular oxygen, mainly including superoxide radicals, hydroxyl radicals, hydrogen peroxide, and singlet oxygen [128]. Moderate levels of ROS can kill bacteria by destroying proteins, lipids, and other components [129,130]. However, the overexpression of ROS will lead to damage to protein and DNA, which may cause cell death and complications like inflammation and fibrosis. Besides, oxidative stress will inhibit cell migration and proliferation and deficiency of GFs [131–135]. Therefore, one effective way to regulate wound healing is to control the level of the ROS [136].

Metals and their oxides are the choice of many researchers for the construction of hydrogel-based dressings with the ability of ROS level regulation. Xie et al. creatively developed an Ångstrom-scale Ag particles-loaded carbomer gel for the treatment of diabetic wounds and large burns. The Ångstrom-scale Ag particles were significantly smaller in scale than commercial Ag NPs and exhibited enhanced ROS generation capacity, effectively inhibiting bacterial colonization and inflammatory response level [137].  $\text{TiO}_2$  is another kind of metal oxide that has both acoustic and photo-sensitivities. You and Yu et al. constructed a gel of amorphous  $\text{TiO}_x$  nanofibers dotted with  $\text{Ti}_2\text{C}(\text{OH})_2$  NSs [138]. This hydrogel could trap the bacteria by forming a Ti-O-P bond between the phosphate

of the bacterial cell wall and Ti-OH, and it could generate sufficient ROS to kill bacteria by combining with exogenous ultrasound radiation. Meanwhile,  $Ti_2C(OH)_2$  in the gel converted  $H_2O_2$  to  $O_2$  and accelerated wound healing.  $TiO_2$  has also been used for antimicrobial photocatalytic therapy. Zhang et al. prepared PF127, PLys, and oxidized HA-based hydrogel with antimicrobial photocatalytic activity by combining  $TiO_2$  NPs and  $LiLuGeO_4:Bi^{3+}$  (LGG) with a UV persistent light-emitting properties [139]. After being stimulated by UV light, LGG emitted light that  $TiO_2$  absorbed to produce persistent ROS, exhibiting long-lasting antimicrobial activity (Figure 7A).

As mentioned above, excessive ROS can cause damage to cell membranes and proteins, impeding tissue regeneration during wound healing processes. Hydrogels with antioxidant capacity are able to control the inflammatory response and accelerate wound healing. Interestingly, Ag NPs can also play an important role in antioxidants. Wang et al. loaded Ag NPs into a DA-gelatin/guar gum-based hydrogel. The obtained hydrogel had excellent antioxidant ability and could scavenge ROS in the wound microenvironment to improve the efficiency of the wound treatment [140]. Nanozymes are NMs that mimic natural enzymes in their reaction mechanism [141]. Ding and Mao et al. prepared a supramolecular hydrogel loaded with hollow mesoporous Prussian blue NPs (HMBPs) [142]. This hydrogel was formed with cyclodextrin (host) and adamantane (guest) modified gellan gums through host-guest interaction. HMBPs were utilized for PTT and to scavenge overexpressed ROS, while the hybrid hydrogel exhibited POD-like activity and SOD-like activity under light irradiation, efficiently relieving oxidative stress and promoting wound healing (Figure 7B). Zhu and Fan et al. developed a gel based on CNTs loaded with  $MoS_2$  NSs. The nanocomplex showed three enzyme-like activities [143]. This hydrogel exhibited peroxidase (POD) activity in an acidic environment and showed superoxide lyase activity and catalase (CAT) activity in a neutral condition. These bioactivities efficiently convert superoxide radicals to  $H_2O_2$  and  $O_2$  and decompose  $H_2O_2$  to  $O_2$ . In addition, the photothermal activity of CNT enhanced the catalytic effect of  $MoS_2$ , and the resulting hydrogel exhibited good free radical scavenging ability (Figure 7C).  $CeO_2$  exhibits excellent ROS redox quenching activity due to the richness of oxygen defects and  $Ce^{3+}$  species [144]. Krebs et al. reported a zwitterionic hydrogel by combining  $CeO_2$  NPs with microRNA, which has anti-inflammatory activity. In this system,  $CeO_2$  NPs acted as an antioxidant to scavenge overexpressed ROS and reduced the level of the inflammatory response by combining with microRNA [145]. Many non-metallic NMs also exhibit great antioxidant potential. Wu and Wang et al. developed a hydrogel using PDA NPs and two natural antioxidant drugs (puerarin and ferulic acid) based on a “the more natural the better” strategy [146]. Under oxidative stress conditions, the hydrogel enhanced superoxide dismutase (SOD) and glutathione peroxidase activities, efficiently scavenged ROS, and reduced malondialdehyde levels. Consequently, the hydrogel circumvented the damage caused by overexpressed ROS. Lu et al. developed a scaffold by incorporating PDA-rGO into a CS/SF-based matrix (pGO-CS/SF) for synergistic antioxidant therapy [147]. The developed bio-scaffold reduced cellular oxidation by removing excess ROS. Meanwhile, this scaffold responded to electrical signals and promoted physiological electrical signals for cell growth to improve tissue regeneration in the wound.

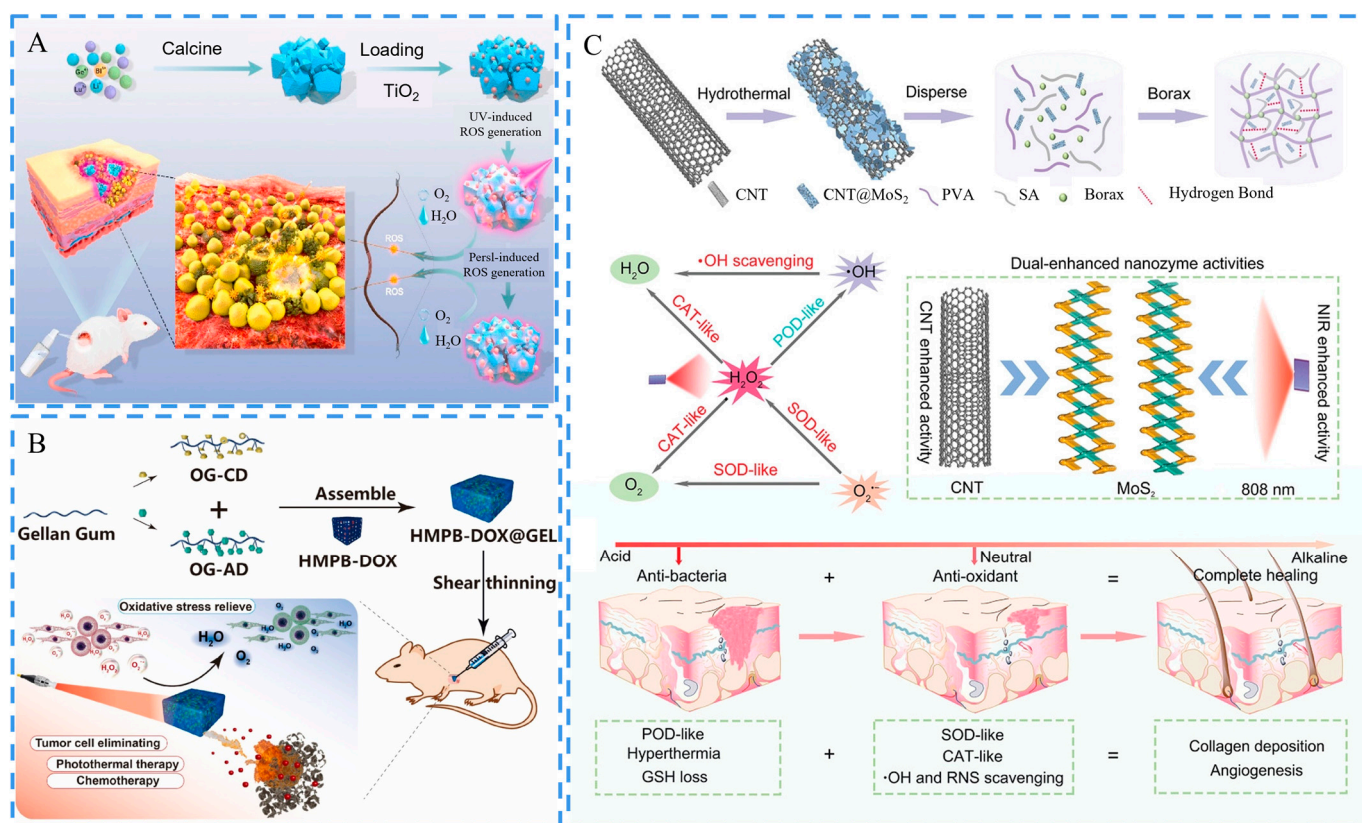


**Figure 7.** Schematics of the ROS-regulating hydrogels. **(A)** Preparation of the antibacterial photocatalyst LGG/TiO<sub>2</sub>-PF127/PLys/oxidized HA-based hydrogel and its application in infected wound healing. Reproduced with permission [139]. Copyright 2021, Elsevier. **(B)** Schematic of the supramolecular hydrogel containing HMPBs loading doxorubicin (HMPB-DOX@GEL) and its application for tumor postoperative treatment. Adapted with permission [142]. Copyright 2022, Elsevier. **(C)** Schematics of the preparation procedure for the CNT@MoS<sub>2</sub> NSs incorporating PVA/SA hydrogel and the summary of CNT and NIR dual-enhanced triple nanozyme activities. Reproduced with permission [143]. Copyright 2021, Wiley-VCH.

### 3.5. Stimulus Responsiveness

#### 3.5.1. Photo-Responsiveness

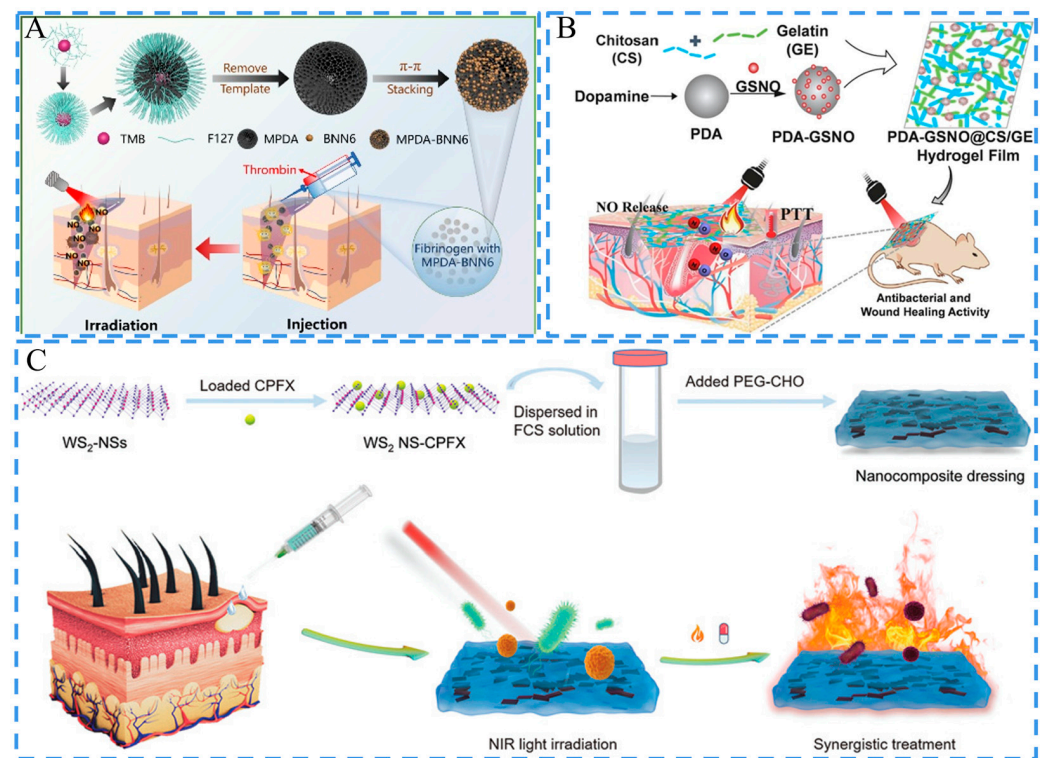
In a spatio-temporal manner, light can regulate some behavior of photo-responsive hydrogels. An adjustable light source with tunable wavelength, power, and duration can be considered a switch to trigger heat production, degradation, or specific biological functions of the hydrogels [148,149].

Photo-responsive hydrogels can be fabricated by introducing NMs with light responsiveness into the gel network [150]. Photothermal therapy (PTT) is a new and emerging treatment method. After the irritation, the absorbed optical energy converts to thermal energy, resulting in the ablation of bacteria via quickly raising the temperature [151]. Additionally, photodynamic therapy (PDT) is based on the photooxidation of the photosensitive dye in the target tissue for the treatment of a wide variety of diseases [152]. It produces few adverse effects and requires a short treatment period [153]. In recent studies, PDA NPs, quantum dots (QDs), porphyrin-based NPs, and some metal-based NPs have been used to construct photo-responsive hydrogels [154–156]. For instance, PDA NPs have been widely utilized in the field of light-related therapies due to the strong light absorption and photothermal conversion efficiency [157,158]. In addition, PDA NPs have also been applied in the development of adhesive hydrogels due to their catechol structure [159]. Yang, Tu, and Dong, et al. encapsulate *N,N'*-disub-butyl-*N,N'*-dinitroso-*p*-phenylenediamine (BNN6)-loaded mesoporous polydopamine (MPDA) in a fibrin gel (MPDA-BNN6 NPs@fibrin)

for the treatment of an infected wound [160]. Under the action of thrombin, soluble fibrinogen was converted into the insoluble fibrin gel after fibrinopeptides were resected from fibrinogen. The hydrogel acted as a light-operated nitric oxide (NO) generator and achieved photothermal/gas dual-modal precise antibacterial therapy under the irradiation of 808 nm light to accelerate bacterial-infected wound closure (Figure 8A). Yang, Ding, and Chen et al. also adapted the strategy to construct a CS/gelatin-based hydrogel with photothermal properties and gas releasing ability [161]. PDA NPs were selected as the photothermal agent, and *S*-nitrosoglutathione (GSNO) was utilized to endow the hydrogel with NO releasing ability. The hydrogel exhibited a local thermal effect and released NO in response to NIR stimulation, resulting in a synergetic strategy for infected wound treatment (Figure 8B). Lu et al. combined PDA NPs with a SF/CS hybrid matrix to construct a bionic gel. In the system, the active catechol groups on the PDA NPs provided multiple bioactive sites for protein and peptide adsorption. The composite gel exerted a potent bactericidal effect under NIR irradiation, thereby modulating the inflammatory response and inhibiting bacterial invasion for wound healing [162]. Li, Huang, and Wu et al. added PDA NPs, GOx, and CAT into a PDA/PAM hydrogel for refractory diabetic wounds. The PDA NPs exhibited an efficient antimicrobial effect under NIR irradiation. The hydrogel could also effectively control blood glucose levels at the wound site due to the introduction of GOx and CAT. Furthermore, the hydrogel could produce sufficient oxygen to support cell proliferation [163].

Carbon quantum dots (CQDs) are another photothermal conversion agent with photoluminescent and free radical scavenging properties [164]. Wu et al. constructed a photo-responsive hydrogel by introducing CQDs and ZnO into a folic acid-conjugated PDA composite system [165]. CQDs could not only generate ROS rapidly but also exert inherent photoresponsivity to achieve 99.9% killing of G+ and G- bacterial under 660 nm and 808 nm light illumination. The Zn<sup>2+</sup> released from the hydrogel also provided a long-lasting antibacterial property and regulated cell behavior by promoting the proliferation of fibroblasts. Das et al. constructed a hydrogel via loading DNA-ligated CNDs into a poly(vinylpyrrolidone) matrix, and the CNDs generated ROS when visible light irradiation for efficient sterilization. In addition, the hydrogel could be used to track drug delivery because the fluorescence of CND would burst in the presence of a heme [166].

Nanozymes have also been applied in photosensitization therapy. Two dimensional MOF nanozymes with ultrathin nano-thickness usually have higher catalytic activity than conventional nanozymes [167]. Wang et al. developed a PEG-based hydrogel loaded with 2D zirconium-ferrocene MOF NPs in combination with PTT for skin wound treatment. The hydrogel exhibited potential synergistic antibacterial effects for the treatment of a bacterially infected skin wound [168]. MoS<sub>2</sub> NM is a 2D material with good biocompatibility and POD-like properties that shows the potential for non-invasive antimicrobial therapy [34]. Additionally, the nano forms of many transition metal elements also have good photo-responsive properties. Cu NPs have a localized surface plasmon resonance effect and can effectively convert NIR irradiant power into local thermal energy for PTT purpose [169]. Cai et al. developed a hydrogel via loading Cu NPs in a matrix based on a copolymer of GelMA and *N,N*-bis(acryloyl)-cystamin. The Cu NPs embedded in the hydrogel produced ROS and converted the excitation energy of NIR into local heat, demonstrating a powerful killing ability against both G+ and G- bacteria [170]. Au and Ag also present the surface plasmon resonance effect. Zhou et al. prepared a hydrogel with photothermal effects by loading Au and Ag hybrid NSs into SH. After laser irradiation, AgAuNSs eradicated *E. coli* and *S. aureus* [171]. Yu et al. co-added WS<sub>2</sub> NSs with the antibiotic ciprofloxacin (CPF) into a matrix based on dodecyl-modified chitosan (FCS) and dialdehyde-functionalized PEG (PEG-CHO) to construct a hydrogel with a photothermal effect and spatio-temporal modulation of drug release [172]. WS<sub>2</sub> generated a large amount of heat under NIR irradiation, which simultaneously triggered the release of antibiotics. The hydrogel and NIR synergistically promoted wound healing and circumvented the shortcomings of the two separate treatment modes (Figure 8C).



**Figure 8.** Schematics of the photo-responsive hydrogels. (A) Schematic of the fabrication and application of the hydrogel MPDA-BNN6@fibrin in anti-infective therapy and wound healing. Reproduced with permission [160]. Copyright 2022, Elsevier. (B) Schematic of synthetic procedure and NIR-triggered PTT and NO therapy of the hydrogel PDA-GSNO@CS/gelatin for enhanced wound healing. Adapted with permission [161]. Copyright 2022, Elsevier. (C) Schematics of the preparation procedure for WS<sub>2</sub>-CPFX/FCS/PEG-CHO hydrogel and the synergistic therapy of an infected wound. Adapted with permission [172]. Copyright 2020, Elsevier.

### 3.5.2. pH Responsiveness

Every biochemical reaction needs to be carried out at an optimal pH. The pH value at the wound site changes dynamically during the healing process, which means the state of wound healing can be monitored and regulated by manipulating the local pH [173]. The optimization of wound healing speed by artificially introducing NMs capable of regulating pH has been studied [174].

Most bacteria produce acetic and lactic acids during multiplication and metabolism in infected wounds, resulting in local acidification (pH 4.5–6.5) [175]. Srivastava et al. loaded a polyelectrolyte-vitamin C nanoparticulate system into a PVA-Alg hydrogel to create an acidic environment around the wound to promote faster closure [176]. Dai and Li et al. loaded Ag NPs in a lignocellulose/SA/PVA network to construct a hydrogel. The acidic environment led to the disruption between Ag and boric acid, generating a longer pH-dependent release behavior of the hydrogel [177]. Wang et al., constructed a dual-cross-linked hydrogel from chitosan, quaternary ammonium salt, and ODEX-DA through the formation of catechol-catechol adducts and the Schiff base reaction [178]. They also opted for Ag NPs as the antimicrobial agent against infectious bacteria in the diabetic wound microenvironment. The acidic environment disrupted the network structure, leading to the responsive release of Ag NPs (Figure 9). Copello et al. developed a keratin hydrogel loaded with ZnO NPs for protection against bacterial infections. The hydrogel shrank under acidic conditions and swelled in response to contact with alkaline media in chronic wounds, thereby releasing NPs that formed an antimicrobial barrier and protected the wound from bacterial infection [179].

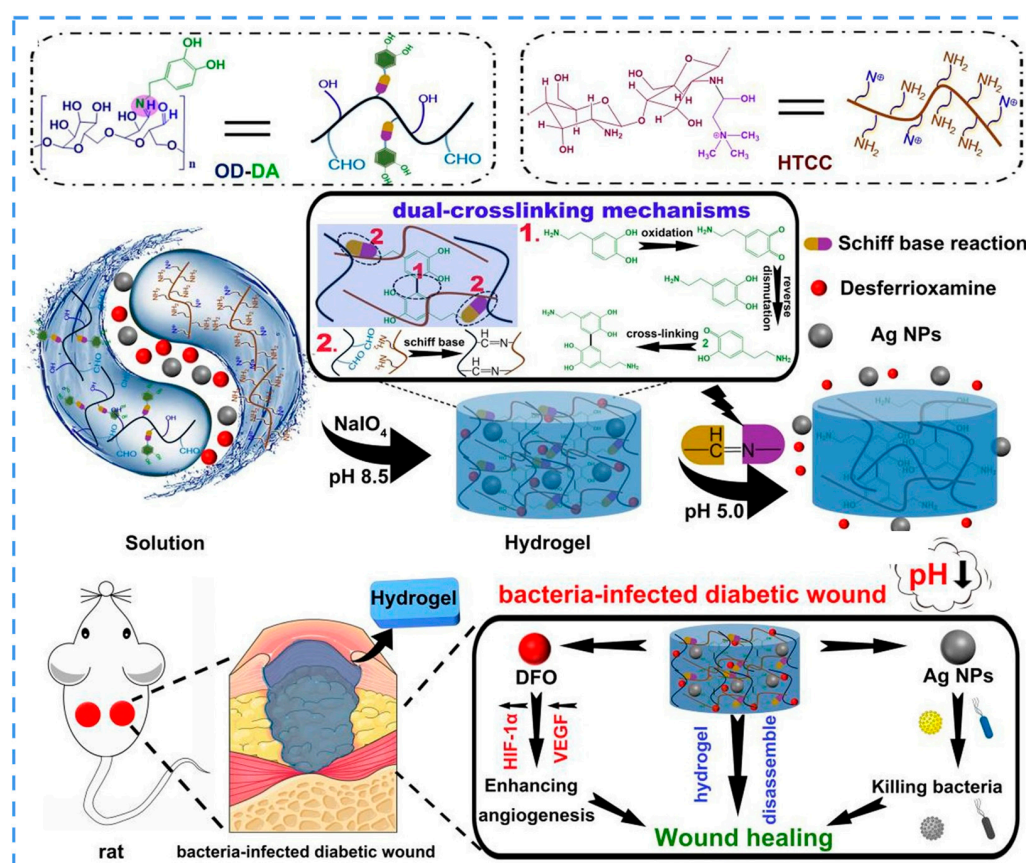


**Figure 9.** Schematics of the formation and mechanisms of hydrogel Ag NPs@HTCC/ODEX-DA (ODEX-DA = OD-DA), and the antibacterial and wound healing mechanisms including enhancing angiogenesis and killing bacteria. Adapted with permission [178]. Copyright 2021, Elsevier.

Changes in pH can regulate the release of the drug by altering the formation and breaking of chemical bonds between the hydrogel network and the drug [180]. Moreover, the gelation and degradation processes of hydrogels can also be controlled by adjusting the pH to manipulate loaded drug release [181]. Zeng et al. constructed an ultrasensitive pH-responsive hydrogel, which formed through the Schiff base reaction between an aldehyde-containing copolymer from 2-methacryloyloxyethyl phosphorylcholine (MPC), 4-formylbenzoate ethyl methacrylate (FBEMA), and amine-modified SiO<sub>2</sub> NPs. In the neutral environment, the pre gel solution could gelatinize rapidly within 10 s. More intelligently, the hydrogel underwent a rapid gel-sol transition to trigger drug release in an acidic environment created by the acute inflammatory response [182]. Liu, Jin, and Xuan et al. constructed a CS hydrogel encapsulating formyl-met-leu-phe (fMLP) and FasL-conjugated silica NPs (SiO<sub>2</sub>-fasL). This hydrogel degraded when it was applied to the wound site because of the acidic microenvironment. The fMLP recruited neutrophils to the wound to initiate an inflammatory reaction, which created an acidic environment. Then the pH-responsive hydrogel matrix began to degrade, and the exposed SiO<sub>2</sub>-fasL triggered FasL-Fas signaling to induce neutrophil apoptosis, promoting the conversion of the anti-inflammatory phenotype of macrophages to drive regeneration. This creative strategy for transient enhancement of the inflammatory response provided a novel solution for the treatment of diabetic skin wound [183].

### 3.5.3. Magnetic Responsiveness

Magnetic responsive hydrogels are highly sensitive to the magnetic field. The integration of magnetic NPs (MNPs) and functional polymer networks can be achieved through electrostatic interaction or hydrogen bonding, such as to Fe<sub>3</sub>O<sub>4</sub> and MnFe<sub>2</sub>O<sub>4</sub> NPs, and

can be introduced into biopolymer networks [184]. The introduction of magnetic materials into the gel network allows the hydrogel to have remotely tunable properties. Furthermore, the magnetic field is an intermediate medium to regulate the delivery and release of the loaded drug without any additional contact, showing great potential for further development of multifunctional hydrogels in the biomedical engineering field [185,186].  $\text{Fe}_3\text{O}_4$  NPs are magnetic NPs with superparamagnetic property [187]. Tan and Chen et al. constructed a polysaccharide-based magnetic hydrogel by encapsulating  $\text{Fe}_3\text{O}_4$  NPs in a carboxymethyl cellulose and CS network. The magnetic microspheres enabled the hydrogel to have a fast and strong response to the external magnetic field, offering the possibility of delivering the loaded drug [188]. Forouzandehdel and Rami et al. prepared an itaconic acid/starch/fucoidan-based hydrogel loaded with a magnetic field responsive  $\text{Fe}_3\text{O}_4$ @graphene sheets nanocomplex and guaifenesin as a wound treatment drug. The hydrogel could achieve on-demand drug delivery under the action of an external magnetic field [189]. This model was also adopted by Sadeghi et al. They used itaconic acid/starch as a hydrogel matrix and selected  $\text{Fe}_3\text{O}_4$  NMs as the magnetic responsive agent to achieve controlled release of the drug under the action of an external magnetic field [190]. This model provides a universal and pervasive platform for responsive controlled release that can be applied not only in the field of wound healing, but also in the treatment of other diseases, and it is worth further study. In addition, Wang et al. fabricated an Alg/poly-*L*-ornithine/gelatin hydrogel sheet with a groove pattern for use as a cell delivery platform [191].  $\text{Fe}_3\text{O}_4$  NPs were incorporated into the patterned hydrogel sheet for the magnetic field-induced transfer of cell-seeded hydrogel sheets. In the meantime, cell differentiation from an endothelial progenitor cell (EPC) to an endothelial cell promoted rapid cell migration and vascularization, thus accelerating wound healing (Figure 10). However, the application of NMs-based magnetic hydrogels in wound healing is not yet widespread, probably because wound management is an emergency treatment and the need for drugs or active ingredients is urgent rather than a postponable treatment.

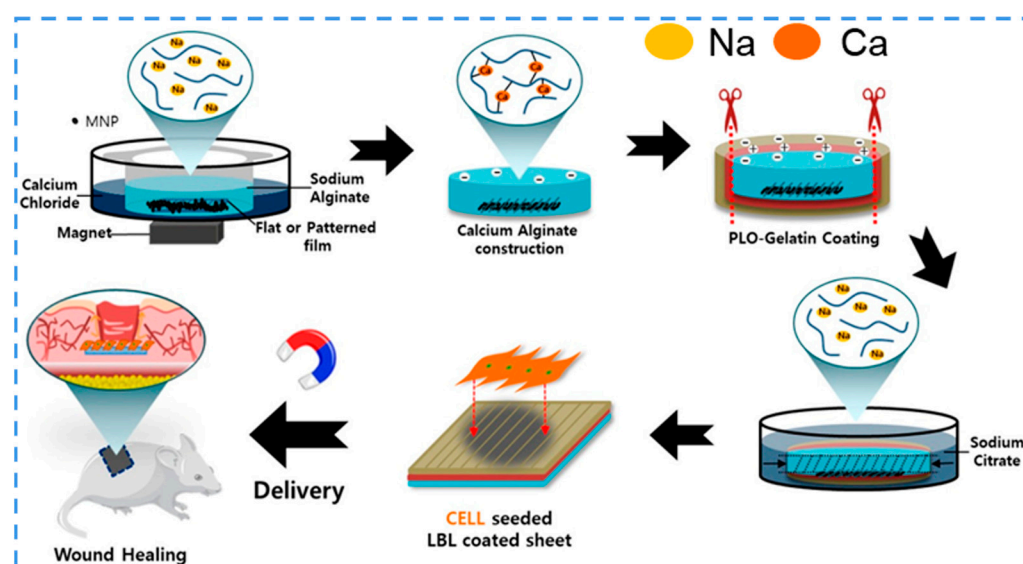


**Figure 10.** Schematic of the synthesis procedure of MNPs-embedded hydrogel sheet with groove pattern for wound healing. Reproduced with permission [191]. Copyright 2019, The American Chemical Society.

A summary table is provided to introduce the other NMFHs that are not mentioned in the text above (Table 1). Several widely studied types including hemostatic, antimicrobial, conductive, and photo-responsive hydrogels are summarized from NMs species, hydrogel matrix, and the mechanisms of specific biological functions.

**Table 1.** Summary of other NMFHs with different functions.

| Function                 | Nanomaterial  | Hydrogel Matrix   | Mechanism  | Ref   |
|--------------------------|---|---|--|-------|
| Hemostatic Ability       | polydopamine decorated Ag NPs (PDA@Ag NPs)              | Oxidized Alg and catechol-modified gelatin  | Good adhesion reduced blood loss and gelatin promoted platelet aggregation.  | [192] |
|                          | GO  | dopamine grafted gelatin (GelDA)  | The catechol group of dopamine (DA) attached to wound and stopped bleeding.  | [193] |
|                          | transferrin conjugated CuO <sub>2</sub> NPs (CP@Tf NPs) | copolymer of <i>N</i> -isopropylacrylamide (NIPAM), acrylamide (Aam), <i>N</i> -[3-(dimethylamino)propyl]-methacrylamide (DMPA), and methylene- <i>N,N</i> -bis(acrylamide) | Abundant amino acid groups of the hydrogel attracted negatively charged red blood cells to gather and form blood clotting, and Cu <sup>2+</sup> promoted coagulation.  | [194] |
|                          | Au NPs  | CS  | Au NPs stimulated the intrinsic coagulation pathway.   | [195] |
|                          | multiwalled carbon nanotubes (MWCNTs)                   | copolymer of glycidyl methacrylate functionalized quaternized-CS (QCSG) and PF127   | MWCNTs trigger platelets activation and Ca <sup>2+</sup> from extracellular activated the release of platelet membrane microparticles.   | [196] |
|                          | nano whitlockite (nWH)                                  | CS  | Various coagulation factors involved in the coagulation cascade were activated by the Ca <sup>2+</sup> , Mg <sup>2+</sup> , and PO <sub>4</sub> <sup>3-</sup> released from nWH and amine groups of CS.                              | [197] |
| Antimicrobial activities | Ag NPs  | galacto-xyloglucan and PAM  | The released Ag <sup>+</sup> affected the replication and/or inactivation of the microbial flora.  | [198] |
|                          | PDA@Ag NPs  | PANI and PVA  | Ag NPs released Ag <sup>+</sup> and bind to bacteria to destroy them.  | [199] |
|                          | Zn doped nWH (Zn-nWH)                                   | copolymer of methacrylate anhydride quaternized CS (QCSMA) and methacrylate anhydride DA (DAMA)   | The Zn <sup>2+</sup> released from Zn-nWH synergizing with QCSMA achieved a high antibacterial effect.   | [200] |
|                          | Cu NPs  | CS/ PF127   | Depolarization of the cell membrane through interaction between the cell membrane and Cu NPs weakened the cell outer membrane, and Cu <sup>2+</sup> penetrated the cell and mediated the ROS to block the bacterial cell metabolism. | [201] |

Table 1. Cont.

| Function     | Nanomaterial                   | Hydrogel Matrix   | Mechanism  | Ref   |
|--------------|--------------------------------|---|--|-------|
|              | GO/CuO nanocomposite           | CS and PVA  | NPs accumulate around bacteria, causing bacterial oxidative stress, DNA damage, and lactate dehydrogenase (LDH) release.                             | [202] |
|              | Ag NPs                         | copolymer of L-DA, PEG, and gelatin (GPLD)                        | Star-shaped topology cationic GPLD with and/or certain functional group on the side chain showed antimicrobial activity.                             | [203] |
|              | TiO <sub>2</sub> NPs or Ag NPs | xylan and CS  | Incorporation of TiO <sub>2</sub> NPs or Ag NPs in the gel matrix provided synergistic effects in killing bacterial.                                 | [204] |
|              | CeO NPs                        | DA-modified GelMA   | CeO NPs cleaned extracellular ROS and prevented intracellular ROS production.  | [205] |
|              | Ag NPs                         | silk fibroin (SF)   | Ag NPs destroyed the bacterial structure and inhibited the inflammatory response.  | [21]  |
|              | Ag NPs                         | porcine dermal decellularized extracellular matrix                | Ag NPs destroyed the structure of bacteria.  | [206] |
|              | reduced graphene oxide (rGO)   | DA modified HA (DA-HA)  | High temperature (above 50°C) could kill bacteria through destroying some enzymes and proteins.  | [8]   |
| Conductivity | CNTs                           | GelMA   | The conductive hydrogel could promote the NE-C4 stem cells proliferation and differentiation.  | [207] |
|              | CNTs                           | DA-gelatin/CS/PDA   | The conductive hydrogel could adjust electrical signals and promote wound healing via improving blood flow, enhancing migration, and reducing edema. | [37]  |
|              | CNTs                           | N-carboxyethyl CS/benzaldehyde-terminated PF127                   | The CNT-based conductive hydrogel showed photothermal ability to shorten the healing process of infected wound.                                      | [114] |
|              | GO-graft-cyclodextrin          | quaternized CS-graft-cyclodextrin/quaternized CS-graft-adamantane | The hydrogel could regulate cell adhesion, proliferation, and migration with/without ES.   | [115] |
|              | TA-chelated Ag NPs             | PAAc  | The conductive hydrogels facilitated the earliest stage of myotube formation.  | [208] |

Table 1. Cont.

| Function             | Nanomaterial  | Hydrogel Matrix                                      | Mechanism  | Ref   |
|----------------------|---|--|--|-------|
| Photo-responsiveness | Ppy NPs   | GelMA/CS-catechol                                    | The conductive hydrogel could regulate cellular behavior and benefit better integration and growth with tissues.   | [209] |
|                      | Ti <sub>3</sub> C <sub>2</sub> T <sub>x</sub> MXene@CeO <sub>2</sub> nanocomposites | Polyethyleneimine grafted-PF127/oxidized SA          | The conductive hydrogel is beneficial to the proliferation and migration of fibroblasts under the ES.  | [210] |
|                      | ZnO QDs@GO  | CS   | ROS, and the Zn <sup>2+</sup> released from ZnO QDs under acid environment killed the bacteria.  | [211] |
|                      | Cu, N-doped carbon dots (Cu, N-CDs)@GO NSs  | CS   | The hydrogel could absorb 808 nm light and convert the energy into thermal energy due to the photothermal effects of Cu, N-CDs, and GO NSs.  | [212] |
|                      | UiO-66-NH <sub>2</sub> MOF NPs  | CS   | The MOF could produce active oxygen ( $\cdot$ OH) by pre-UV-irradiation or in the presence of a trace amount of H <sub>2</sub> O <sub>2</sub> to kill the bacteria.                    | [213] |
|                      | berberine chloride NPs  | N-(9-fluorenylmethoxycarbonyl)-L-phenylalanine       | The hydrogel exhibited AIE behavior and <sup>1</sup> O <sub>2</sub> generation under white light, and kill bacteria via a PDT mechanism, and in turn penetrate and eradicate biofilms. | [214] |
|                      | black phosphorus QDs (BPQDs)  | PVA/Alg  | BPQDs were photo responsive, ROS-generating, and antibacterial, which could promote the MRSA-infected wound healing.   | [215] |
|                      | catechol-modified CS-derived carbonized polymer dots (CPDs)                         | PVA  | The PVA@CPDs hydrogel could reach the desired temperature quickly under irradiation, thus efficiently killing the bacteria and preventing overheating of normal tissues.               | [216] |
|                      | PANI NPs  | PAM  | The hydrogel could convert light energy into heat upon NIR irradiation and be used as a photothermal antibacterial material.   | [45]  |
|                      | Ppy NTs   | quaternized CS-graft- $\beta$ -cyclodextrin, adenine | The PTT enhanced wound healing by promoting collagen deposition.   | [217] |

#### 4. Conclusions and Perspectives

Hydrogels for the treatment of cutaneous wounds have shown tremendous growth in recent decades, and the nanomaterials functionalized hydrogels (NMFHs) perform better in this area. The excellent physical, chemical, and biological properties of nanomaterials (NMs) provide a wide range of opportunities for the targeted functionalization of hydrogels. As one of the most conventional and convenient modification methods, loading NMs can confer diverse functions on the hydrogels, such as hemostasis, antimicrobial activity, conductivity, and the ability to regulate ROS levels. In addition, with the rise of smart hydrogels in recent years, NMs are playing an increasingly important role in the development of stimulus-responsive (pH responsive, photo-responsive, and magnetic responsive) hydrogels. The development of NMs-based stimulus-responsive hydrogels is valuable because such intelligent material can modulate behaviors of the hydrogels by exogenous modifiable means, allowing the release of the internal active ingredients on demand [218–221]. Precisely, programmed administration is more beneficial for active ingredient release [222].

However, there are some challenges to the development of NMFHs in the wound dressing field, where the creation of multifunctional hydrogels is meaningful when applying them to complex wound scenarios. Hence, it is necessary to select modifiers that can perform multiple biological functions, mobilize the body's own repair potential, and activate the production of endogenous active substances to achieve better healing results. In these scenarios, the hydrogels can be artificially modified by selecting cell-derived proteins, such as growth factors (GFs), chemokines, or nucleic acid sequences with specific biological functions to be grafted onto the NMs. Secondly, the biocompatibility of the hydrogels should be further improved, and systematic evaluations need to be performed to promote their clinical applications. Thirdly, the mechanical properties of some hydrogels should be improved to ensure the healing efficiency of the materials during the whole healing process. The process of wound healing is complex, including variations in mechanical properties and cell behaviors. Moreover, tissue structure and mechanical forces are important signals for cell decision making, and the forces are constantly transferred between the extracellular machinery matrix and intercellular adhesion sites. The key is the mechanical changes caused by the cell and the ECM, as well as the forces generated in the cell and exerted by the outside world [223,224]. Therefore, NMFHs with controllable mechanical strength are desirable. Besides, stem cell therapy is an emerging therapy for cutaneous wound treatment, and its application to wounds based on NMFHs is a bright prospect. Stimulus-responsive NMFHs may be able to regulate the fate of loaded stem cells under physicochemical stimulations, thus avoiding the inevitable side effects caused by the introduction of exogenous proteins or chemical inducers [225,226].

In conclusion, NMFHs have significant research and application values in skin wound dressings. To address the expanding and complex problem of wound repair and lessen the suffering of patients, cutaneous wound hydrogel dressings will be developed in the future with improved biocompatibility, better repair effects, and a higher degree of bionic mimicry. It is hoped that this review will inspire researchers to generate more creative ideas and concepts in the field of NMFHs for cutaneous wound healing.

**Author Contributions:** Conceptualization, Z.L.; writing—original draft preparation, Y.L.; writing—review and editing, Y.L., G.S. and Z.L.; supervision, Z.L. and R.D.; project administration, Z.L., R.Z. and R.D.; funding acquisition, Z.L. and R.Z. All authors have read and agreed to the published version of the manuscript.

**Funding:** This review was funded by the National Natural Science Foundation of China (22005028, 22105020), and Beijing Institute of Technology Research Fund Program for Young Scholars (XSQD-202023002, XSQD-202123005).

**Institutional Review Board Statement:** Not applicable.

**Informed Consent Statement:** Not applicable.

**Data Availability Statement:** Not applicable.

**Conflicts of Interest:** The authors declare no conflict of interest.

## References

1. Li, H.J.; Gao, G.R.; Xu, Z.Y.; Tang, D.N.; Chen, T. Recent Progress in Bionic Skin Based on Conductive Polymer Gels. *Macromol. Rapid Commun.* **2021**, *42*, 2100480. [[CrossRef](#)]
2. Liang, Y.; He, J.; Guo, B. Functional Hydrogels as Wound Dressing to Enhance Wound Healing. *ACS Nano* **2021**, *15*, 12687–12722. [[CrossRef](#)] [[PubMed](#)]
3. Van, D.; Bogdanov, B.; Rooze, N.D.; Sch Ac Ht, E.H.; Cornelissen, M.; Berghmans, H. Structural and rheological properties of methacrylamide modified gelatin hydrogels. *Biomacromolecules* **2000**, *1*, 31–38.
4. Cubo, N.; Garcia, M.; Canizo, J.D.; Velasco, D.; Jorcano, J.L. 3D bioprinting of functional human skin: Production and in vivo analysis. *Biofabrication* **2017**, *9*, 2843–2854. [[CrossRef](#)] [[PubMed](#)]
5. Jarbrink, K.; Ni, G.; Sonnergren, H.; Schmidtchen, A.; Pang, C.; Bajpai, R.; Car, J. The humanistic and economic burden of chronic wounds: A protocol for a systematic review. *Syst. Rev.* **2017**, *6*, 7. [[CrossRef](#)]
6. Yannas, I.V.; Burke, J.F.; Orgill, D.P.; Skrabut, E.M. Wound tissue can utilize a polymeric template to synthesize a functional extension of skin. *Science* **1982**, *215*, 174–176. [[CrossRef](#)]
7. Ji, X.; Li, Z.; Hu, Y.; Xie, H.; Wu, W.; Song, F.; Liu, H.; Wang, J.; Jiang, M.; Lam, J.W.Y.; et al. Bioinspired Hydrogels with Muscle-Like Structure for AIEgen-Guided Selective Self-Healing. *CCS Chem.* **2021**, *3*, 1146–1156. [[CrossRef](#)]
8. Liang, Y.P.; Zhao, X.; Hu, T.L.; Chen, B.J.; Yin, Z.H.; Ma, P.X.; Guo, B.L. Adhesive Hemostatic Conducting Injectable Composite Hydrogels with Sustained Drug Release and Photothermal Antibacterial Activity to Promote Full-Thickness Skin Regeneration During Wound Healing. *Small* **2019**, *15*, e1900046. [[CrossRef](#)]
9. Ghobril, C.; Charoen, K.; Rodriguez, E.K.; Nazarian, A.; Grinstaff, M.W. A Dendritic Thioester Hydrogel Based on Thiol-Thioester Exchange as a Dissolvable Sealant System for Wound Closure. *Angew. Chem.-Int. Ed.* **2013**, *52*, 14070–14074. [[CrossRef](#)]
10. Hu, H.; Xu, F.J. Rational design and latest advances of polysaccharide-based hydrogels for wound healing. *Biomater. Sci.* **2020**, *8*, 2084–2101. [[CrossRef](#)]
11. Wang, S.G.; Wang, F.; Shi, K.; Yuan, J.F.; Sun, W.L.; Yang, J.T.; Chen, Y.X.; Zhang, D.; Che, L.B. Osteichthyes skin-inspired tough and sticky composite hydrogels for dynamic adhesive dressings. *Compos. Part B-Eng.* **2022**, *241*, 110010. [[CrossRef](#)]
12. Sun, G.M.; Zhang, X.J.; Shen, Y.I.; Sebastian, R.; Dickinson, L.E.; Fox-Talbot, K.; Reinblatt, M.; Steenbergen, C.; Harmon, J.W.; Gerecht, S. Dextran hydrogel scaffolds enhance angiogenic responses and promote complete skin regeneration during burn wound healing. *Proc. Natl. Acad. Sci. USA* **2011**, *108*, 20976–20981. [[CrossRef](#)] [[PubMed](#)]
13. Saatchi, A.; Arani, A.R.; Moghanian, A.; Mozafari, M. Cerium-doped bioactive glass-loaded chitosan/polyethylene oxide nanofiber with elevated antibacterial properties as a potential wound dressing. *Ceram. Int.* **2021**, *47*, 9447–9461. [[CrossRef](#)]
14. Griffin, D.R.; Weaver, W.M.; Scumpia, P.O.; Di Carlo, D.; Segura, T. Accelerated wound healing by injectable microporous gel scaffolds assembled from annealed building blocks. *Nat. Mater.* **2015**, *14*, 737–744. [[CrossRef](#)]
15. Jannesari, M.; Varshosaz, J.; Morshed, M.; Zamani, M. Composite poly(vinyl alcohol)/poly(vinyl acetate) electrospun nanofibrous mats as a novel wound dressing matrix for controlled release of drugs. *Int. J. Nanomed.* **2011**, *6*, 993–1003. [[CrossRef](#)]
16. He, J.H.; Liang, Y.P.; Shi, M.T.; Guo, B.L. Anti-oxidant electroactive and antibacterial nanofibrous wound dressings based on poly(epsilon-caprolactone)/quaternized chitosan-graft-polyaniline for full-thickness skin wound healing. *Chem. Eng. J.* **2020**, *385*, 123464. [[CrossRef](#)]
17. Augustine, R.; Rehman, S.R.U.; Ahmed, R.; Zahid, A.A.; Sharifi, M.; Falahati, M.; Hasan, A. Electrospun chitosan membranes containing bioactive and therapeutic agents for enhanced wound healing. *Int. J. Biol. Macromol.* **2020**, *156*, 153–170. [[CrossRef](#)]
18. Feng, Y.F.; Li, X.F.; Zhang, Q.; Yan, S.Q.; Guo, Y.; Li, M.Z.; You, R.C. Mechanically robust and flexible silk protein/polysaccharide composite sponges for wound dressing. *Carbohydr. Polym.* **2019**, *216*, 17–24. [[CrossRef](#)]
19. Li, D.W.; Tao, L.; Wu, T.; Wang, L.L.; Sun, B.B.; Ke, Q.F.; Mo, X.M.; Deng, B.Y. Mechanically-reinforced 3D scaffold constructed by silk nonwoven fabric and silk fibroin sponge. *Colloids Surf. B-Biointerfaces* **2020**, *196*, 111361. [[CrossRef](#)]
20. Rameshbabu, A.P.; Bankoti, K.; Datta, S.; Subramani, E.; Apoorva, A.; Ghosh, P.; Maity, P.P.; Manchikanti, P.; Chaudhury, K.; Dhara, S. Silk Sponges Ornamented with a Placenta-Derived Extracellular Matrix Augment Full-Thickness Cutaneous Wound Healing by Stimulating Neovascularization and Cellular Migration. *ACS Appl. Mater. Interfaces* **2018**, *10*, 16977–16991. [[CrossRef](#)]
21. Liu, Y.K.; Fan, J.C.; Lv, M.Q.; She, K.P.; Sun, J.L.; Lu, Q.Q.; Han, C.H.; Ding, S.T.; Zhao, S.; Wang, G.X.; et al. Photocrosslinking silver nanoparticles-aloe vera-silk fibroin composite hydrogel for treatment of full-thickness cutaneous wounds. *Regen. Biomater.* **2021**, *8*, rbab048. [[CrossRef](#)] [[PubMed](#)]
22. Liang, Y.Q.; Li, Z.L.; Huang, Y.; Yu, R.; Guo, B.L. Dual-Dynamic-Bond Cross-Linked Antibacterial Adhesive Hydrogel Sealants with On-Demand Removability for Post-Wound-Closure and Infected Wound Healing. *ACS Nano* **2021**, *15*, 7078–7093. [[CrossRef](#)] [[PubMed](#)]
23. Sheng, L.L.; Zhang, Z.W.B.; Zhang, Y.; Wang, E.D.; Ma, B.; Xu, Q.; Ma, L.L.; Zhang, M.; Pei, G.; Chang, J. A novel “hot spring”-mimetic hydrogel with excellent angiogenic properties for chronic wound healing. *Biomaterials* **2021**, *264*, 120414. [[CrossRef](#)] [[PubMed](#)]

24. Balakrishnan, B.; Mohanty, M.; Umashankar, P.R.; Jayakrishnan, A. Evaluation of an in situ forming hydrogel wound dressing based on oxidized alginate and gelatin. *Biomaterials* **2005**, *26*, 6335–6342. [[CrossRef](#)]
25. Xuan, Q.Z.; Jiang, F.; Dong, H.; Zhang, W.X.; Zhang, F.Y.; Ma, T.H.; Zhuang, J.F.; Yu, J.L.; Wang, Y.B.; Shen, H.; et al. Bioinspired Intrinsic Versatile Hydrogel Fabricated by Amyloid Toxin Simulant-Based Nanofibrous Assemblies for Accelerated Diabetic Wound Healing. *Adv. Funct. Mater.* **2021**, *31*, 2106705. [[CrossRef](#)]
26. Qi, J.; Su, G.; Li, Z. Gel-Based Luminescent Conductive Materials and Their Applications in Biosensors and Bioelectronics. *Materials* **2021**, *14*, 6759. [[CrossRef](#)]
27. Su, G.; Li, Z.; Dai, R. Recent Advances in Applied Fluorescent Polymeric Gels. *ACS Appl. Polym. Mater.* **2022**, *4*, 3131–3152. [[CrossRef](#)]
28. Liu, D.P.; Yin, G.Q.; Le, X.X.; Chen, T. Supramolecular topological hydrogels: From material design to applications. *Polym. Chem.* **2022**, *13*, 1940–1952. [[CrossRef](#)]
29. Li, Z.; Ji, X.; Xie, H.; Tang, B.Z. Aggregation-Induced Emission-Active Gels: Fabrications, Functions, and Applications. *Adv. Mater.* **2021**, *33*, e2100021. [[CrossRef](#)]
30. Liu, H.; Wei, S.X.; Qiu, H.Y.; Si, M.Q.; Lin, G.Q.; Lei, Z.K.; Lu, W.; Zhou, L.; Chen, T. Supramolecular Hydrogel with Orthogonally Responsive R/G/B Fluorophores Enables Multi-Color Switchable Biomimetic Soft Skins. *Adv. Funct. Mater.* **2022**, *32*, 2108830. [[CrossRef](#)]
31. Sabbagh, F.; Muhamad, I.I.; Niazmand, R.; Dikshit, P.K.; Kim, B.S. Recent progress in polymeric non-invasive insulin delivery. *Int. J. Biol. Macromol.* **2022**, *203*, 222–243. [[CrossRef](#)] [[PubMed](#)]
32. Khan, I.; Saeed, K.; Khan, I. Nanoparticles: Properties, applications and toxicities. *Arab. J. Chem.* **2019**, *12*, 908–931. [[CrossRef](#)]
33. Boomi, P.; Ganesan, R.M.; Poorani, G.; Prabu, H.G.; Ravikumar, S.; Jeyakanthan, J. Biological synergy of greener gold nanoparticles by using *Coleus aromaticus* leaf extract. *Mater. Sci. Eng. C-Mater. Biol. Appl.* **2019**, *99*, 202–210. [[CrossRef](#)] [[PubMed](#)]
34. Yang, S.; Zang, G.; Peng, Q.; Fan, J.; Liu, Y.; Zhang, G.; Zhao, Y.; Li, H.; Zhang, Y. In-situ growth of 3D rosette-like copper nanoparticles on carbon cloth for enhanced sensing of ammonia based on copper electrodisolution. *Anal. Chim. Acta* **2020**, *1104*, 60–68. [[CrossRef](#)] [[PubMed](#)]
35. Peng, Q.; Zhang, Y.; Yang, S.; Yuwen, T.; Liu, Y.; Fan, J.; Zang, G. Glucose determination behaviour of gold microspheres-electrodeposited carbon cloth flexible electrodes in neutral media. *Anal. Chim. Acta* **2021**, *1159*, 338442. [[CrossRef](#)] [[PubMed](#)]
36. Sankar, R.; Baskaran, A.; Shivashangari, K.S.; Ravikumar, V. Inhibition of pathogenic bacterial growth on excision wound by green synthesized copper oxide nanoparticles leads to accelerated wound healing activity in Wistar Albino rats. *J. Mater. Sci.-Mater. Med.* **2015**, *26*, 214. [[CrossRef](#)] [[PubMed](#)]
37. Liang, Y.P.; Zhao, X.; Hu, T.L.; Han, Y.; Guo, B.L. Mussel-inspired, antibacterial, conductive, antioxidant, injectable composite hydrogel wound dressing to promote the regeneration of infected skin. *J. Colloid Interface Sci.* **2019**, *556*, 514–528. [[CrossRef](#)]
38. Zou, M.Z.; Liu, W.L.; Chen, H.S.; Bai, X.F.; Gao, F.; Ye, J.J.; Cheng, H.; Zhang, X.Z. Advances in nanomaterials for treatment of hypoxic tumor. *Natl. Sci. Rev.* **2021**, *8*, nwaa160. [[CrossRef](#)]
39. Huang, S.; Hong, X.; Zhao, M.; Liu, N.; Liu, H.; Zhao, J.; Shao, L.; Xue, W.; Zhang, H.; Zhu, P.; et al. Nanocomposite hydrogels for biomedical applications. *Bioeng. Transl. Med.* **2022**, *7*, e10315. [[CrossRef](#)]
40. Yah, C.S.; Simate, G.S. Nanoparticles as potential new generation broad spectrum antimicrobial agents. *Daru* **2015**, *23*, 43. [[CrossRef](#)]
41. Stoica, A.E.; Chircov, C.; Grumezescu, A.M. Nanomaterials for Wound Dressings: An Up-to-Date Overview. *Molecules* **2020**, *25*, 2699. [[CrossRef](#)] [[PubMed](#)]
42. Chen, K.; Wang, F.; Liu, S.; Wu, X.; Xu, L.; Zhang, D. In situ reduction of silver nanoparticles by sodium alginate to obtain silver-loaded composite wound dressing with enhanced mechanical and antimicrobial property. *Int. J. Biol. Macromol.* **2020**, *148*, 501–509. [[CrossRef](#)] [[PubMed](#)]
43. Fan, Y.; Wu, W.; Lei, Y.; Gaucher, C.; Pei, S.; Zhang, J.; Xia, X. Edaravone-Loaded Alginate-Based Nanocomposite Hydrogel Accelerated Chronic Wound Healing in Diabetic Mice. *Mar. Drugs* **2019**, *17*, 285. [[CrossRef](#)] [[PubMed](#)]
44. Linhart, A.N.; Wortman-Otto, K.M.; Deninger, I.; Dudek, A.L.; Lange, H.R.; Danhausen, D.M.; Graverson, C.F.; Beckmann, T.J.; Havens, M.A.; Keleher, J.J. Strategic Design of Antimicrobial Hydrogels Containing Biomimetic Additives for Enhanced Matrix Responsiveness and HDFa Wound Healing Rates. *ACS Appl. Bio Mater.* **2020**, *3*, 5750–5758. [[CrossRef](#)]
45. Pang, Q.; Wu, K.H.; Jiang, Z.L.; Shi, Z.W.; Si, Z.Z.; Wang, Q.; Cao, Y.H.; Hou, R.X.; Zhu, Y.B. A Polyaniline Nanoparticles Crosslinked Hydrogel with Excellent Photothermal Antibacterial and Mechanical Properties for Wound Dressing. *Macromol. Biosci.* **2022**, *22*, 2100386. [[CrossRef](#)] [[PubMed](#)]
46. Ding, T.; Qi, J.; Zou, J.; Dan, H.; Zhao, H.; Chen, Q. A multifunctional supramolecular hydrogel for infected wound healing. *Biomater. Sci.* **2022**, *10*, 381–395. [[CrossRef](#)]
47. Hong, Y.; Zhou, F.F.; Hua, Y.J.; Zhang, X.Z.; Ni, C.Y.; Pan, D.H.; Zhang, Y.Q.; Jiang, D.M.; Yang, L.; Lin, Q.N.; et al. A strongly adhesive hemostatic hydrogel for the repair of arterial and heart bleeds. *Nat. Commun.* **2019**, *10*, 2060. [[CrossRef](#)]
48. Clarke, D.L.; Quazi, M.A.; Reddy, K.; Thomson, S.R. Emergency operation for penetrating thoracic trauma in a metropolitan surgical service in South Africa. *J. Thorac. Cardiovasc. Surg.* **2011**, *142*, 563–568. [[CrossRef](#)]
49. Dong, R.N.; Zhang, H.L.; Guo, B.L. Emerging hemostatic materials for non-compressible hemorrhage control. *Natl. Sci. Rev.* **2022**, *9*, nwac162. [[CrossRef](#)]

50. Gaston, E.; Fraser, J.F.; Xu, Z.P.; Ta, H.T. Nano- and micro-materials in the treatment of internal bleeding and uncontrolled hemorrhage. *Nanomedicine* **2018**, *14*, 507–519. [[CrossRef](#)]
51. Guo, B.; Dong, R.; Liang, Y.; Li, M. Haemostatic materials for wound healing applications. *Nat. Rev. Chem.* **2021**, *5*, 773–791. [[CrossRef](#)]
52. Zhang, Y.S.; Khademhosseini, A. Advances in engineering hydrogels. *Science* **2017**, *356*, eaaf3627. [[CrossRef](#)] [[PubMed](#)]
53. Li, Z.W.; Lu, W.; Ngai, T.; Le, X.X.; Zheng, J.; Zhao, N.; Huang, Y.J.; Wen, X.F.; Zhang, J.W.; Chen, T. Mussel-inspired multifunctional supramolecular hydrogels with self-healing, shape memory and adhesive properties. *Polym. Chem.* **2016**, *7*, 5343–5346. [[CrossRef](#)]
54. Sun, Z.; Chen, X.Y.; Ma, X.M.; Cui, X.X.; Yi, Z.; Li, X.D. Cellulose/keratin-catechin nanocomposite hydrogel for wound hemostasis. *J. Mater. Chem. B* **2018**, *6*, 6133–6141. [[CrossRef](#)] [[PubMed](#)]
55. Li, Z.; Li, B.; Li, X.; Lin, Z.; Chen, L.; Chen, H.; Jin, Y.; Zhang, T.; Xia, H.; Lu, Y.; et al. Ultrafast in-situ forming halloysite nanotube-doped chitosan/oxidized dextran hydrogels for hemostasis and wound repair. *Carbohydr. Polym.* **2021**, *267*, 118155. [[CrossRef](#)] [[PubMed](#)]
56. Ryu, J.H.; Hong, S.; Lee, H. Bio-inspired adhesive catechol-conjugated chitosan for biomedical applications: A mini review. *Acta Biomater.* **2015**, *27*, 101–115. [[CrossRef](#)]
57. Lin, J.; Wang, M.; Hu, H.; Yang, X.; Wen, B.; Wang, Z.; Jacobson, O.; Song, J.; Zhang, G.; Niu, G.; et al. Multimodal-Imaging-Guided Cancer Phototherapy by Versatile Biomimetic Theranostics with UV and gamma-Irradiation Protection. *Adv. Mater.* **2016**, *28*, 3273–3279. [[CrossRef](#)]
58. Li, M.; Liang, Y.; Liang, Y.; Pan, G.; Guo, B. Injectable stretchable self-healing dual dynamic network hydrogel as adhesive anti-oxidant wound dressing for photothermal clearance of bacteria and promoting wound healing of MRSA infected motion wounds. *Chem. Eng. J.* **2022**, *427*, 132039. [[CrossRef](#)]
59. Lan, G.; Li, Q.; Lu, F.; Yu, K.; Lu, B.; Bao, R.; Dai, F. Improvement of platelet aggregation and rapid induction of hemostasis in chitosan dressing using silver nanoparticles. *Cellulose* **2019**, *27*, 385–400. [[CrossRef](#)]
60. Jun, E.A.; Lim, K.M.; Kim, K.; Bae, O.N.; Noh, J.Y.; Chung, K.H.; Chung, J.H. Silver nanoparticles enhance thrombus formation through increased platelet aggregation and procoagulant activity. *Nanotoxicology* **2011**, *5*, 157–167. [[CrossRef](#)]
61. Hattori, H.; Ishihara, M. Feasibility of improving platelet-rich plasma therapy by using chitosan with high platelet activation ability. *Exp. Ther. Med.* **2017**, *13*, 1176–1180. [[CrossRef](#)] [[PubMed](#)]
62. Zhang, M.; Wang, D.; Ji, N.; Lee, S.; Wang, G.; Zheng, Y.; Zhang, X.; Yang, L.; Qin, Z.; Yang, Y. Bioinspired Design of Sericin/Chitosan/Ag@MOF/GO Hydrogels for Efficiently Combating Resistant Bacteria, Rapid Hemostasis, and Wound Healing. *Polymers* **2021**, *13*, 2812. [[CrossRef](#)]
63. Xiong, Y.; Chen, L.; Liu, P.; Yu, T.; Lin, C.; Yan, C.; Hu, Y.; Zhou, W.; Sun, Y.; Panayi, A.C.; et al. All-in-One: Multifunctional Hydrogel Accelerates Oxidative Diabetic Wound Healing through Timed-Release of Exosome and Fibroblast Growth Factor. *Small* **2022**, *18*, e2104229. [[CrossRef](#)] [[PubMed](#)]
64. Sundaram, M.N.; Amirthalingam, S.; Mony, U.; Varma, P.K.; Jayakumar, R. Injectable chitosan-nano bioglass composite hemostatic hydrogel for effective bleeding control. *Int. J. Biol. Macromol.* **2019**, *129*, 936–943. [[CrossRef](#)] [[PubMed](#)]
65. Chen, J.Y.; He, J.H.; Yang, Y.T.; Qiao, L.P.; Hu, J.; Zhang, J.; Guo, B.L. Antibacterial adhesive self-healing hydrogels to promote diabetic wound healing. *Acta Biomater.* **2022**, *146*, 119–130. [[CrossRef](#)]
66. Liang, Y.; Liang, Y.; Zhang, H.; Guo, B. Antibacterial biomaterials for skin wound dressing. *Asian J. Pharm. Sci.* **2022**, *17*, 353–384. [[CrossRef](#)]
67. Rafique, A.; Mahmood Zia, K.; Zuber, M.; Tabasum, S.; Rehman, S. Chitosan functionalized poly(vinyl alcohol) for prospects biomedical and industrial applications: A review. *Int. J. Biol. Macromol.* **2016**, *87*, 141–154. [[CrossRef](#)]
68. Zhao, P.; Feng, Y.; Zhou, Y.; Tan, C.; Liu, M. Gold@Halloysite nanotubes-chitin composite hydrogel with antibacterial and hemostatic activity for wound healing. *Bioact. Mater.* **2023**, *20*, 355–367. [[CrossRef](#)]
69. Aderibigbe, B.A.; Buyana, B. Alginate in Wound Dressings. *Pharmaceutics* **2018**, *10*, 42. [[CrossRef](#)]
70. Khamrai, M.; Banerjee, S.L.; Paul, S.; Samanta, S.; Kundu, P.P. Curcumin entrapped gelatin/ionically modified bacterial cellulose based self-healable hydrogel film: An eco-friendly sustainable synthesis method of wound healing patch. *Int. J. Biol. Macromol.* **2019**, *122*, 940–953. [[CrossRef](#)]
71. Geisberger, G.; Gyenge, E.B.; Hinger, D.; Kach, A.; Maake, C.; Patzke, G.R. Chitosan-Thioglycolic Acid as a Versatile Antimicrobial Agent. *Biomacromolecules* **2013**, *14*, 1010–1017. [[CrossRef](#)] [[PubMed](#)]
72. Zhao, X.; Li, P.; Guo, B.L.; Ma, P.X. Antibacterial and conductive injectable hydrogels based on quaternized chitosan-graft-polyaniline/oxidized dextran for tissue engineering. *Acta Biomater.* **2015**, *26*, 236–248. [[CrossRef](#)] [[PubMed](#)]
73. Sun, J.; Tan, H.; Liu, H.; Jin, D.; Yin, M.; Lin, H.; Qu, X.; Liu, C. A reduced polydopamine nanoparticle-coupled sprayable PEG hydrogel adhesive with anti-infection activity for rapid wound sealing. *Biomater. Sci.* **2020**, *8*, 6946–6956. [[CrossRef](#)] [[PubMed](#)]
74. Yuan, J.; Zhang, D.; He, X.; Ni, Y.; Che, L.; Wu, J.; Wu, B.; Wang, Y.; Wang, S.; Sha, D.; et al. Cationic peptide-based salt-responsive antibacterial hydrogel dressings for wound healing. *Int. J. Biol. Macromol.* **2021**, *190*, 754–762. [[CrossRef](#)] [[PubMed](#)]
75. Dai, Z.; Zhang, Y.; Chen, C.; Yu, F.; Tian, J.; Cai, H.; Jiang, X.; Zhang, L.; Zhang, W. An Antifouling and Antimicrobial Zwitterionic Nanocomposite Hydrogel Dressing for Enhanced Wound Healing. *ACS Biomater. Sci. Eng.* **2021**, *7*, 1621–1630. [[CrossRef](#)]
76. Bakhsheshi-Rad, H.R.; Ismail, A.F.; Aziz, M.; Akbari, M.; Hadisi, Z.; Omid, M.; Chen, X. Development of the PVA/CS nanofibers containing silk protein sericin as a wound dressing: In vitro and in vivo assessment. *Int. J. Biol. Macromol.* **2020**, *149*, 513–521. [[CrossRef](#)]

77. Huang, S.; Chen, H.-J.; Deng, Y.-P.; You, X.-H.; Fang, Q.-h.; Lin, M. Preparation of novel stable microbicidal hydrogel films as potential wound dressing. *Polym. Degrad. Stabil.* **2020**, *181*, 109349. [[CrossRef](#)]
78. Diab, S.E.; Tayea, N.A.; Elwakil, B.H.; Gad, A.A.M.; Ghareeb, D.A.; Olama, Z.A. Novel Amoxicillin-Loaded Sericin Biopolymeric Nanoparticles: Synthesis, Optimization, Antibacterial and Wound Healing Activities. *Int. J. Mol. Sci.* **2022**, *23*, 11654. [[CrossRef](#)]
79. Song, K.; Hao, Y.; Liu, Y.; Cao, R.; Zhang, X.; He, S.; Wen, J.; Zheng, W.; Wang, L.; Zhang, Y. Preparation of pectin-chitosan hydrogels based on bioadhesive-design micelle to prompt bacterial infection wound healing. *Carbohydr. Polym.* **2023**, *300*, 120272. [[CrossRef](#)]
80. Lara, H.H.; Garza-Trevino, E.N.; Ixtepan-Turrent, L.; Singh, D.K. Silver nanoparticles are broad-spectrum bactericidal and virucidal compounds. *J. Nanobiotechnol.* **2011**, *9*, 30. [[CrossRef](#)]
81. Tang, S.; Zheng, J. Antibacterial Activity of Silver Nanoparticles: Structural Effects. *Adv. Healthc. Mater.* **2018**, *7*, e1701503. [[CrossRef](#)] [[PubMed](#)]
82. Yin, I.X.; Zhang, J.; Zhao, I.S.; Mei, M.L.; Li, Q.; Chu, C.H. The Antibacterial Mechanism of Silver Nanoparticles and Its Application in Dentistry. *Int. J. Nanomed.* **2020**, *15*, 2555–2562. [[CrossRef](#)] [[PubMed](#)]
83. Paladini, F.; Pollini, M. Antimicrobial Silver Nanoparticles for Wound Healing Application: Progress and Future Trends. *Materials* **2019**, *12*, 2540. [[CrossRef](#)] [[PubMed](#)]
84. Ovais, M.; Ahmad, I.; Khalil, A.T.; Mukherjee, S.; Javed, R.; Ayaz, M.; Raza, A.; Shinwari, Z.K. Wound healing applications of biogenic colloidal silver and gold nanoparticles: Recent trends and future prospects. *Appl. Microbiol. Biotechnol.* **2018**, *102*, 4305–4318. [[CrossRef](#)] [[PubMed](#)]
85. Jiang, Y.; Huang, J.; Wu, X.; Ren, Y.; Li, Z.; Ren, J. Controlled release of silver ions from AgNPs using a hydrogel based on konjac glucomannan and chitosan for infected wounds. *Int. J. Biol. Macromol.* **2020**, *149*, 148–157. [[CrossRef](#)]
86. Fan, Z.J.; Liu, B.; Wang, J.Q.; Zhang, S.Y.; Lin, Q.Q.; Gong, P.W.; Ma, L.M.; Yang, S.R. A Novel Wound Dressing Based on Ag/Graphene Polymer Hydrogel: Effectively Kill Bacteria and Accelerate Wound Healing. *Adv. Funct. Mater.* **2014**, *24*, 3933–3943. [[CrossRef](#)]
87. Tian, Y.; Tatsuma, T. Mechanisms and applications of plasmon-induced charge separation at TiO<sub>2</sub> films loaded with gold nanoparticles. *J. Am. Chem. Soc.* **2005**, *127*, 7632–7637. [[CrossRef](#)]
88. Wang, J.; Zhang, C.; Yang, Y.; Fan, A.; Chi, R.; Shi, J.; Zhang, X. Poly (vinyl alcohol) (PVA) hydrogel incorporated with Ag/TiO<sub>2</sub> for rapid sterilization by photoinspired radical oxygen species and promotion of wound healing. *Appl. Surf. Sci.* **2019**, *494*, 708–720. [[CrossRef](#)]
89. Shi, G.; Chen, W.; Zhang, Y.; Dai, X.; Zhang, X.; Wu, Z. An Antifouling Hydrogel Containing Silver Nanoparticles for Modulating the Therapeutic Immune Response in Chronic Wound Healing. *Langmuir* **2019**, *35*, 1837–1845. [[CrossRef](#)]
90. Ghasemi, A.H.; Farazin, A.; Mohammadimehr, M.; Naeimi, H. Fabrication and characterization of biopolymers with antibacterial nanoparticles and Calendula officinalis flower extract as an active ingredient for modern hydrogel wound dressings. *Mater. Today Commun.* **2022**, *31*, 103513. [[CrossRef](#)]
91. Ahmed, A.; Niazi, M.B.K.; Jahan, Z.; Ahmad, T.; Hussain, A.; Pervaiz, E.; Janjua, H.A.; Hussain, Z. In-vitro and in-vivo study of superabsorbent PVA/Starch/g-C<sub>3</sub>N<sub>4</sub>/Ag@TiO<sub>2</sub> NPs hydrogel membranes for wound dressing. *Eur. Polym. J.* **2020**, *130*, 109650. [[CrossRef](#)]
92. Ragothaman, M.; Kannan Villalan, A.; Dhanasekaran, A.; Palanisamy, T. Bio-hybrid hydrogel comprising collagen-capped silver nanoparticles and melatonin for accelerated tissue regeneration in skin defects. *Mater. Sci. Eng. C Mater. Biol. Appl.* **2021**, *128*, 112328. [[CrossRef](#)] [[PubMed](#)]
93. Wang, X.C.; Li, G.H.; Ding, Y.; Sun, S.Q. Understanding the photothermal effect of gold nanostars and nanorods for biomedical applications. *RSC Adv.* **2014**, *4*, 30375–30383. [[CrossRef](#)]
94. Majumder, S.; Ranjan Dahiya, U.; Yadav, S.; Sharma, P.; Ghosh, D.; Rao, G.K.; Rawat, V.; Kumar, G.; Kumar, A.; Srivastava, C.M. Zinc Oxide Nanoparticles Functionalized on Hydrogel Grafted Silk Fibroin Fabrics as Efficient Composite Dressing. *Biomolecules* **2020**, *10*, 710. [[CrossRef](#)]
95. Zhang, M.; Qiao, X.N.; Han, W.W.; Jiang, T.Z.; Liu, F.; Zhao, X. Alginate-chitosan oligosaccharide-ZnO composite hydrogel for accelerating wound healing. *Carbohydr. Polym.* **2021**, *266*, 118100. [[CrossRef](#)]
96. Tang, L.; Zhu, L.; Tang, F.; Yao, C.; Wang, J.; Li, L. Mild Synthesis of Copper Nanoparticles with Enhanced Oxidative Stability and Their Application in Antibacterial Films. *Langmuir* **2018**, *34*, 14570–14576. [[CrossRef](#)]
97. Zhang, K.X.; Zhao, G.Y. An Effective Wound Healing Material Based on Gold Incorporation into a Heparin-Polyvinyl Alcohol Nanocomposite: Enhanced In Vitro and In Vivo Care of Perioperative Period. *J. Clust. Sci.* **2021**, *33*, 1655–1665. [[CrossRef](#)]
98. Abdollahi, Z.; Zare, E.N.; Salimi, F.; Goudarzi, I.; Tay, F.R.; Makvandi, P. Bioactive Carboxymethyl Starch-Based Hydrogels Decorated with CuO Nanoparticles: Antioxidant and Antimicrobial Properties and Accelerated Wound Healing In Vivo. *Int. J. Mol. Sci.* **2021**, *22*, 2531. [[CrossRef](#)]
99. Huang, T.; Yuan, B.; Jiang, W.; Ding, Y.; Jiang, L.; Ren, H.; Tang, J. Glucose oxidase and Fe<sub>3</sub>O<sub>4</sub>/TiO<sub>2</sub>/Ag<sub>3</sub>PO<sub>4</sub> co-embedded biomimetic mineralization hydrogels as controllable ROS generators for accelerating diabetic wound healing. *J. Mater. Chem. B* **2021**, *9*, 6190–6200. [[CrossRef](#)]
100. Deuel, H.; Neukom, H.; Weber, F. Reaction of boric acid with polysaccharides. *Nature* **1948**, *161*, 96–97. [[CrossRef](#)]
101. Li, X.; Yang, X.; Wang, Z.; Liu, Y.; Guo, J.; Zhu, Y.; Shao, J.; Li, J.; Wang, L.; Wang, K. Antibacterial, antioxidant and biocompatible nanosized quercetin-PVA xerogel films for wound dressing. *Colloids Surf. B Biointerfaces* **2022**, *209*, 112175. [[CrossRef](#)] [[PubMed](#)]

102. Xi, J.; Wu, Q.; Xu, Z.; Wang, Y.; Zhu, B.; Fan, L.; Gao, L. Aloe-Emodin/Carbon Nanoparticle Hybrid Gels with Light-Induced and Long-Term Antibacterial Activity. *ACS Biomater. Sci. Eng.* **2018**, *4*, 4391–4400. [[CrossRef](#)] [[PubMed](#)]
103. Reczynska-Kolman, K.; Hartman, K.; Kwiecien, K.; Brzychczy-Wloch, M.; Pamula, E. Composites Based on Gellan Gum, Alginate and Nisin-Enriched Lipid Nanoparticles for the Treatment of Infected Wounds. *Int. J. Mol. Sci.* **2021**, *23*, 321. [[CrossRef](#)] [[PubMed](#)]
104. Lu, Y.H.; Wang, Y.A.; Zhang, J.Y.; Hu, X.F.; Yang, Z.Y.; Guo, Y.; Wang, Y.B. In-situ doping of a conductive hydrogel with low protein absorption and bacterial adhesion for electrical stimulation of chronic wounds. *Acta Biomater.* **2019**, *89*, 217–226. [[CrossRef](#)]
105. Hammer, B.E. Physical Properties of Tissues. *Mosc. Univ. Math. Bull.* **1991**, *54*, 128. [[CrossRef](#)]
106. So, J.Y.; Lee, J.; Ahn, Y.; Kang, D.; Bae, W.G. The synergistic effect of biomimetic electrical stimulation and extracellular-matrix-mimetic nanopattern for upregulating cell activities. *Biosens. Bioelectron.* **2020**, *167*, 112470. [[CrossRef](#)]
107. Rouabhia, M.; Park, H.; Meng, S.; Derbali, H.; Zhang, Z. Electrical stimulation promotes wound healing by enhancing dermal fibroblast activity and promoting myofibroblast transdifferentiation. *PLoS ONE* **2013**, *8*, e71660. [[CrossRef](#)]
108. Huttenlocher, A.; Horwitz, A.R. Wound Healing with Electric Potential. *N. Engl. J. Med.* **2007**, *356*, 303–304. [[CrossRef](#)]
109. Talikowska, M.; Fu, X.X.; Lisak, G. Application of conducting polymers to wound care and skin tissue engineering: A review. *Biosens. Bioelectron.* **2019**, *135*, 50–63. [[CrossRef](#)]
110. Kargozar, S.; Baino, F.; Hamzehlou, S.; Hamblin, M.R.; Mozafari, M. Nanotechnology for angiogenesis: Opportunities and challenges. *Chem. Soc. Rev.* **2020**, *49*, 5008–5057. [[CrossRef](#)]
111. Yu, R.; Li, Z.L.; Pan, G.Y.; Guo, B.L. Antibacterial conductive self-healable supramolecular hydrogel dressing for infected motional wound healing. *Sci. China-Chem.* **2022**, *65*, 2238–2251. [[CrossRef](#)]
112. Liang, Y.; Xiao, P.; Wang, S.; Shi, J.W.; He, J.; Zhang, J.W.; Huang, Y.J.; Chen, T. Scalable fabrication of free-standing, stretchable CNT/TPE ultrathin composite films for skin adhesive epidermal electronics. *J. Mater. Chem. C* **2018**, *6*, 6666–6671. [[CrossRef](#)]
113. Zheng, M.; Wang, X.; Yue, O.; Hou, M.; Zhang, H.; Beyer, S.; Blocki, A.M.; Wang, Q.; Gong, G.; Liu, X.; et al. Skin-inspired gelatin-based flexible bio-electronic hydrogel for wound healing promotion and motion sensing. *Biomaterials* **2021**, *276*, 121026. [[CrossRef](#)]
114. He, J.H.; Shi, M.T.; Liang, Y.P.; Guo, B.L. Conductive adhesive self-healing nanocomposite hydrogel wound dressing for photothermal therapy of infected full-thickness skin wounds. *Chem. Eng. J.* **2020**, *394*, 124888. [[CrossRef](#)]
115. Zhang, B.; He, J.; Shi, M.; Liang, Y.; Guo, B. Injectable self-healing supramolecular hydrogels with conductivity and photo-thermal antibacterial activity to enhance complete skin regeneration. *Chem. Eng. J.* **2020**, *400*, 125994. [[CrossRef](#)]
116. Faroni, A.; Mobasseri, S.A.; Kingham, P.J.; Reid, A.J. Peripheral nerve regeneration: Experimental strategies and future perspectives. *Adv. Drug Deliv. Rev.* **2015**, *82–83*, 160–167. [[CrossRef](#)]
117. Scheib, J.; Höke, A. Advances in peripheral nerve regeneration. *Nat. Rev. Neurol.* **2013**, *9*, 668–676. [[CrossRef](#)]
118. Tan, M.H.; Xu, X.H.; Yuan, T.J.; Hou, X.; Wang, J.; Jiang, Z.H.; Peng, L.H. Self-powered smart patch promotes skin nerve regeneration and sensation restoration by delivering biological-electrical signals in program. *Biomaterials* **2022**, *283*, 121413. [[CrossRef](#)]
119. Wang, C.; Jiang, X.; Kim, H.J.; Zhang, S.; Zhou, X.; Chen, Y.; Ling, H.; Xue, Y.; Chen, Z.; Qu, M.; et al. Flexible patch with printable and antibacterial conductive hydrogel electrodes for accelerated wound healing. *Biomaterials* **2022**, *285*, 121479. [[CrossRef](#)]
120. Deng, P.P.; Chen, F.X.; Zhang, H.D.; Chen, Y.; Zhou, J.P. Conductive, Self-Healing, Adhesive, and Antibacterial Hydrogels Based on Lignin/Cellulose for Rapid MRSA-Infected Wound Repairing. *ACS Appl. Mater. Interfaces* **2021**, *13*, 52333–52345. [[CrossRef](#)]
121. Zhou, L.; Zheng, H.; Liu, Z.; Wang, S.; Liu, Z.; Chen, F.; Kong, J.; Zhou, F.; Zhang, Q. Conductive Antibacterial Hemostatic Multifunctional Scaffolds Based on Ti3C2Tx MXene Nanosheets for Promoting Multidrug-Resistant Bacteria-Infected Wound Healing. *ACS Nano* **2021**, *15*, 2468–2480. [[CrossRef](#)] [[PubMed](#)]
122. Fan, L.; Xiao, C.; Guan, P.; Zou, Y.; Wen, H.; Liu, C.; Luo, Y.; Tan, G.; Wang, Q.; Li, Y.; et al. Extracellular Matrix-Based Conductive Interpenetrating Network Hydrogels with Enhanced Neurovascular Regeneration Properties for Diabetic Wounds Repair. *Adv. Healthc. Mater.* **2022**, *11*, e2101556. [[CrossRef](#)] [[PubMed](#)]
123. Du, S.; Suo, H.; Xie, G.; Lyu, Q.; Mo, M.; Xie, Z.; Zhou, N.; Zhang, L.; Tao, J.; Zhu, J. Self-powered and photothermal electronic skin patches for accelerating wound healing. *Nano Energy* **2022**, *93*, 106906. [[CrossRef](#)]
124. Yang, K.; Xu, H.; Cheng, L.; Sun, C.Y.; Wang, J.; Liu, Z. In Vitro and In Vivo Near-Infrared Photothermal Therapy of Cancer Using Polypyrrole Organic Nanoparticles. *Adv. Mater.* **2012**, *24*, 5586–5592. [[CrossRef](#)] [[PubMed](#)]
125. Cai, S.; Xu, X.J.; Yang, W.; Chen, J.X.; Fang, X.S. Materials and Designs for Wearable Photodetectors. *Adv. Mater.* **2019**, *31*, e1808138. [[CrossRef](#)] [[PubMed](#)]
126. Wu, C.; Shen, L.; Lu, Y.; Hu, C.; Liang, Z.; Long, L.; Ning, N.; Chen, J.; Guo, Y.; Yang, Z.; et al. Intrinsic Antibacterial and Conductive Hydrogels Based on the Distinct Bactericidal Effect of Polyaniline for Infected Chronic Wound Healing. *ACS Appl. Mater. Interfaces* **2021**, *13*, 52308–52320. [[CrossRef](#)] [[PubMed](#)]
127. Qu, J.; Zhao, X.; Liang, Y.; Xu, Y.; Ma, P.X.; Guo, B. Degradable conductive injectable hydrogels as novel antibacterial, anti-oxidant wound dressings for wound healing. *Chem. Eng. J.* **2019**, *362*, 548–560. [[CrossRef](#)]
128. Trachootham, D.; Alexandre, J.; Huang, P. Targeting cancer cells by ROS-mediated mechanisms: A radical therapeutic approach? *Nat. Rev. Drug Discov.* **2009**, *8*, 579–591. [[CrossRef](#)]
129. Nimse, S.B.; Pal, D. Free radicals, natural antioxidants, and their reaction mechanisms. *RSC Adv.* **2015**, *5*, 27986–28006. [[CrossRef](#)]
130. Finkel, T.; Holbrook, N.J. Oxidants, oxidative stress and the biology of ageing. *Nature* **2000**, *408*, 239–247. [[CrossRef](#)]

131. Guo, J.S.; Sun, W.; Kim, J.P.; Lu, X.L.; Li, Q.Y.; Lin, M.; Mrowczynski, O.; Rizk, E.B.; Cheng, J.G.; Qian, G.Y.; et al. Development of tannin-inspired antimicrobial bioadhesives. *Acta Biomater.* **2018**, *72*, 35–44. [[CrossRef](#)] [[PubMed](#)]
132. Grice, E.A.; Snitkin, E.S.; Yockey, L.J.; Bermudez, D.M.; Liechty, K.W.; Segre, J.A.; Sequencing, N.C. Longitudinal shift in diabetic wound microbiota correlates with prolonged skin defense response. *Proc. Natl. Acad. Sci. USA* **2010**, *107*, 14799–14804. [[CrossRef](#)] [[PubMed](#)]
133. Ma, C.Y.; Tian, X.G.; Kim, J.P.; Xie, D.H.; Ao, X.; Shan, D.Y.; Lin, Q.L.; Hudock, M.R.; Bai, X.C.; Yang, J. Citrate-based materials fuel human stem cells by metabonegenic regulation. *Proc. Natl. Acad. Sci. USA* **2018**, *115*, E11741–E11750. [[CrossRef](#)] [[PubMed](#)]
134. Rodrigues, M.; Kosaric, N.; Bonham, C.A.; Gurtner, G.C. Wound healing: A cellular perspective. *Physiol. Rev.* **2019**, *99*, 665–706. [[CrossRef](#)]
135. Yuan, L.; Sheng, X.; Clark, L.H.; Lu, Z.; Bae-Jump, V.L. Glutaminase inhibitor compound 968 inhibits cell proliferation and sensitizes paclitaxel in ovarian cancer. *Am. J. Transl. Res.* **2016**, *8*, 4265–4277. [[PubMed](#)]
136. Yang, Y.; Liang, Y.; Chen, J.; Duan, X.; Guo, B. Mussel-inspired adhesive antioxidant antibacterial hemostatic composite hydrogel wound dressing via photo-polymerization for infected skin wound healing. *Bioact. Mater.* **2022**, *8*, 341–354. [[CrossRef](#)] [[PubMed](#)]
137. Chen, C.Y.; Yin, H.; Chen, X.; Chen, T.H.; Liu, H.M.; Rao, S.S.; Tan, Y.J.; Qian, Y.X.; Liu, Y.W.; Hu, X.K.; et al. Angstrom-scale silver particle-embedded carbomer gel promotes wound healing by inhibiting bacterial colonization and inflammation. *Sci. Adv.* **2020**, *6*, eaba0942. [[CrossRef](#)]
138. Zhu, Y.-Q.; Huang, W.-Q.; Chen, G.; Xia, L.; You, Y.-Z.; Yu, Y. Sticking-bacteria gel enhancing anti-multidrug-resistant microbial therapy under ultrasound. *Nano Res.* **2022**, *15*, 9105–9113. [[CrossRef](#)]
139. Liu, L.; Shi, J.; Sun, X.; Zhang, Y.; Qin, J.; Peng, S.; Xu, J.; Song, L.; Zhang, Y. Thermo-responsive hydrogel-supported antibacterial material with persistent photocatalytic activity for continuous sterilization and wound healing. *Compos. Part B Eng.* **2022**, *229*, 109459. [[CrossRef](#)]
140. Zhang, H.; Sun, X.; Wang, J.; Zhang, Y.; Dong, M.; Bu, T.; Li, L.; Liu, Y.; Wang, L. Multifunctional Injectable Hydrogel Dressings for Effectively Accelerating Wound Healing: Enhancing Biomineralization Strategy. *Adv. Funct. Mater.* **2021**, *31*, 2100093. [[CrossRef](#)]
141. Zhang, X.J.; Lin, S.J.; Liu, S.W.; Tan, X.L.; Dai, Y.; Xia, F. Advances in organometallic/organic nanozymes and their applications. *Coord. Chem. Rev.* **2021**, *429*, 213652. [[CrossRef](#)]
142. Tong, Z.; Guo, Q.; Xu, G.; Gao, Y.; Yang, H.; Ding, Y.; Wang, W.; Mao, Z. Supramolecular hydrogel-loaded Prussian blue nanoparticles with photothermal and ROS scavenging ability for tumor postoperative treatments. *Compos. Part B Eng.* **2022**, *237*, 109872. [[CrossRef](#)]
143. Li, Y.; Fu, R.; Duan, Z.; Zhu, C.; Fan, D. Adaptive Hydrogels Based on Nanozyme with Dual-Enhanced Triple Enzyme-Like Activities for Wound Disinfection and Mimicking Antioxidant Defense System. *Adv. Healthc Mater.* **2022**, *11*, e2101849. [[CrossRef](#)] [[PubMed](#)]
144. Kim, D.W.; Le, T.M.D.; Lee, S.M.; Kim, H.J.; Ko, Y.J.; Jeong, J.H.; Thambi, T.; Lee, D.S.; Son, S.U. Microporous Organic Nanoparticles Anchoring CeO<sub>2</sub> Materials: Reduced Toxicity and Efficient Reactive Oxygen Species-Scavenging for Regenerative Wound Healing. *ChemNanoMat* **2020**, *6*, 1104–1110. [[CrossRef](#)]
145. Sener, G.; Hilton, S.A.; Osmond, M.J.; Zgheib, C.; Newsom, J.P.; Dewberry, L.; Singh, S.; Sakthivel, T.S.; Seal, S.; Liechty, K.W.; et al. Injectable, self-healable zwitterionic cryogels with sustained microRNA-cerium oxide nanoparticle release promote accelerated wound healing. *Acta Biomater.* **2020**, *101*, 262–272. [[CrossRef](#)]
146. Ou, Q.; Zhang, S.; Fu, C.; Yu, L.; Xin, P.; Gu, Z.; Cao, Z.; Wu, J.; Wang, Y. More natural more better: Triple natural anti-oxidant puerarin/ferulic acid/polydopamine incorporated hydrogel for wound healing. *J. Nanobiotechnol.* **2021**, *19*, 237. [[CrossRef](#)]
147. Tang, P.; Han, L.; Li, P.; Jia, Z.; Wang, K.; Zhang, H.; Tan, H.; Guo, T.; Lu, X. Mussel-Inspired Electroactive and Antioxidative Scaffolds with Incorporation of Polydopamine-Reduced Graphene Oxide for Enhancing Skin Wound Healing. *ACS Appl. Mater. Interfaces* **2019**, *11*, 7703–7714. [[CrossRef](#)]
148. Ramanan, V.V.; Katz, J.S.; Guvendiren, M.; Cohen, E.R.; Marklein, R.A.; Burdick, J.A. Photocleavable side groups to spatially alter hydrogel properties and cellular interactions. *J. Mater. Chem.* **2010**, *20*, 8920–8926. [[CrossRef](#)]
149. Ruskowitz, E.R.; DeForest, C.A. Photoresponsive biomaterials for targeted drug delivery and 4D cell culture. *Nat. Rev. Mater.* **2018**, *3*, 17087. [[CrossRef](#)]
150. Dong, H.; Yang, K.; Zhang, Y.; Li, Q.; Xiu, W.; Ding, M.; Shan, J.; Mou, Y. Photocatalytic Cu<sub>2</sub>WS<sub>4</sub> Nanocrystals for Efficient Bacterial Killing and Biofilm Disruption. *Int. J. Nanomed.* **2022**, *17*, 2735–2750. [[CrossRef](#)]
151. Wang, Y.F.; Meng, H.M.; Song, G.S.; Li, Z.H.; Zhang, X.B. Conjugated-Polymer-Based Nanomaterials for Photothermal Therapy. *ACS Appl. Polym. Mater.* **2020**, *2*, 4258–4272. [[CrossRef](#)]
152. Rajendran, M. Quinones as photosensitizer for photodynamic therapy: ROS generation, mechanism and detection methods. *Photodiagnosis Photodyn. Ther.* **2016**, *13*, 175–187. [[CrossRef](#)] [[PubMed](#)]
153. Choi, J.; Sun, I.C.; Hwang, H.S.; Yoon, H.Y.; Kim, K. Light-triggered photodynamic nanomedicines for overcoming localized therapeutic efficacy in cancer treatment. *Adv. Drug Deliv. Rev.* **2022**, *186*, 114344. [[CrossRef](#)] [[PubMed](#)]
154. Panda, S.; ChawPattnayak, B.; Dash, P.; Nayak, B.; Mohapatra, S. Papaya-Derived Carbon-Dot-Loaded Fluorescent Hydrogel for NIR-Stimulated Photochemotherapy and Antibacterial Activity. *ACS Appl. Polym. Mater.* **2021**, *4*, 369–380. [[CrossRef](#)]
155. Belali, S.; Karimi, A.R.; Hadizadeh, M. Cell-specific and pH-sensitive nanostructure hydrogel based on chitosan as a photosensitizer carrier for selective photodynamic therapy. *Int. J. Biol. Macromol.* **2018**, *110*, 437–448. [[CrossRef](#)]

156. Kumari, S.; Sharma, N.; Sahi, S.V. Advances in Cancer Therapeutics: Conventional Thermal Therapy to Nanotechnology-Based Photothermal Therapy. *Pharmaceutics* **2021**, *13*, 1174. [[CrossRef](#)]
157. Li, Y.Y.; Jiang, C.H.; Zhang, D.W.; Wang, Y.; Ren, X.Y.; Ai, K.L.; Chen, X.S.; Lu, L.H. Targeted polydopamine nanoparticles enable photoacoustic imaging guided chemo-photothermal synergistic therapy of tumor. *Acta Biomater.* **2017**, *47*, 124–134. [[CrossRef](#)]
158. Jin, A.T.; Wang, Y.T.; Lin, K.L.; Jiang, L. Nanoparticles modified by polydopamine: Working as “drug” carriers. *Bioact. Mater.* **2020**, *5*, 522–541. [[CrossRef](#)]
159. Han, L.; Lu, X.; Liu, K.Z.; Wang, K.F.; Fang, L.M.; Weng, L.T.; Zhang, H.P.; Tang, Y.H.; Ren, F.Z.; Zhao, C.C.; et al. Mussel-Inspired Adhesive and Tough Hydrogel Based on Nanoclay Confined Dopamine Polymerization. *ACS Nano* **2017**, *11*, 2561–2574. [[CrossRef](#)]
160. Lv, X.; Xu, Y.; Ruan, X.; Yang, D.; Shao, J.; Hu, Y.; Wang, W.; Cai, Y.; Tu, Y.; Dong, X. An injectable and biodegradable hydrogel incorporated with photoregulated NO generators to heal MRSA-infected wounds. *Acta Biomater.* **2022**, *146*, 107–118. [[CrossRef](#)]
161. Wang, W.; Sheng, H.; Cao, D.; Zhang, F.; Zhang, W.; Yan, F.; Ding, D.; Cheng, N. S-nitrosoglutathione functionalized polydopamine nanoparticles incorporated into chitosan/gelatin hydrogel films with NIR-controlled photothermal/NO-releasing therapy for enhanced wound healing. *Int. J. Biol. Macromol.* **2022**, *200*, 77–86. [[CrossRef](#)] [[PubMed](#)]
162. Han, L.; Li, P.; Tang, P.; Wang, X.; Zhou, T.; Wang, K.; Ren, F.; Guo, T.; Lu, X. Mussel-inspired cryogels for promoting wound regeneration through photobiostimulation, modulating inflammatory responses and suppressing bacterial invasion. *Nanoscale* **2019**, *11*, 15846–15861. [[CrossRef](#)]
163. Wang, Q.; Qiu, W.; Liu, H.; Li, X.; Qin, X.; Wang, X.; Yu, J.; Li, B.; Li, F.; Huang, L.; et al. Conductive hydrogel dressings based on cascade reactions with photothermal effect for monitoring and treatment of diabetic wounds. *Compos. Part B Eng.* **2022**, *242*, 110098. [[CrossRef](#)]
164. Das, B.; Dadhich, P.; Pal, P.; Dhara, S. Single step synthesized sulfur and nitrogen doped carbon nanodots from whey protein: Nanoprobes for longterm cell tracking crossing the barrier of photo-toxicity. *RSC Adv.* **2016**, *6*, 60794–60805. [[CrossRef](#)]
165. Xiang, Y.; Mao, C.; Liu, X.; Cui, Z.; Jing, D.; Yang, X.; Liang, Y.; Li, Z.; Zhu, S.; Zheng, Y.; et al. Rapid and Superior Bacteria Killing of Carbon Quantum Dots/ZnO Decorated Injectable Folic Acid-Conjugated PDA Hydrogel through Dual-Light Triggered ROS and Membrane Permeability. *Small* **2019**, *15*, e1900322. [[CrossRef](#)]
166. Nayak, S.; Prasad, S.R.; Mandal, D.; Das, P. Hybrid DNA-Carbon Dot-Poly(vinylpyrrolidone) Hydrogel with Self-Healing and Shape Memory Properties for Simultaneous Trackable Drug Delivery and Visible-Light-Induced Antimicrobial Photodynamic Inactivation. *ACS Appl. Bio Mater.* **2020**, *3*, 7865–7875. [[CrossRef](#)] [[PubMed](#)]
167. Hu, W.C.; Younis, M.R.; Zhou, Y.; Wang, C.; Xia, X.H. In Situ Fabrication of Ultrasmall Gold Nanoparticles/2D MOFs Hybrid as Nanozyme for Antibacterial Therapy. *Small* **2020**, *16*, e2000553. [[CrossRef](#)] [[PubMed](#)]
168. Wang, X.; Sun, X.; Bu, T.; Wang, Q.; Zhang, H.; Jia, P.; Li, L.; Wang, L. Construction of a photothermal hydrogel platform with two-dimensional PEG@zirconium-ferrocene MOF nanozymes for rapid tissue repair of bacteria-infected wounds. *Acta Biomater.* **2021**, *135*, 342–355. [[CrossRef](#)]
169. Qiu, Y.C.; Leung, S.F.; Wei, Z.H.; Lin, Q.F.; Zheng, X.L.; Zhang, Y.G.; Fan, Z.Y.; Yang, S.H. Enhanced Charge Collection for Splitting of Water Enabled by an Engineered Three-Dimensional Nanospine Array. *J. Phys. Chem. C* **2014**, *118*, 22465–22472. [[CrossRef](#)]
170. Tao, B.; Lin, C.; Deng, Y.; Yuan, Z.; Shen, X.; Chen, M.; He, Y.; Peng, Z.; Hu, Y.; Cai, K. Copper-nanoparticle-embedded hydrogel for killing bacteria and promoting wound healing with photothermal therapy. *J. Mater. Chem B* **2019**, *7*, 2534–2548. [[CrossRef](#)] [[PubMed](#)]
171. He, J.; Qiao, Y.; Zhang, H.; Zhao, J.; Li, W.; Xie, T.; Zhong, D.; Wei, Q.; Hua, S.; Yu, Y.; et al. Gold-silver nanoshells promote wound healing from drug-resistant bacteria infection and enable monitoring via surface-enhanced Raman scattering imaging. *Biomaterials* **2020**, *234*, 119763. [[CrossRef](#)] [[PubMed](#)]
172. Yang, N.; Zhu, M.; Xu, G.; Liu, N.; Yu, C. A near-infrared light-responsive multifunctional nanocomposite hydrogel for efficient and synergistic antibacterial wound therapy and healing promotion. *J. Mater. Chem B* **2020**, *8*, 3908–3917. [[CrossRef](#)] [[PubMed](#)]
173. McArdle, C.; Lagan, K.M.; McDowell, D.A. The pH of wound fluid in diabetic foot ulcers—the way forward in detecting clinical infection? *Curr. Diabetes Rev.* **2014**, *10*, 177–181. [[CrossRef](#)] [[PubMed](#)]
174. Cui, T.; Yu, J.; Wang, C.F.; Chen, S.; Li, Q.; Guo, K.; Qing, R.; Wang, G.; Ren, J. Micro-Gel Ensembles for Accelerated Healing of Chronic Wound via pH Regulation. *Adv. Sci.* **2022**, *9*, e2201254. [[CrossRef](#)]
175. Lu, Y.M.; Wu, Y.; Liang, J.; Libera, M.R.; Sukhishvili, S.A. Self-defensive antibacterial layer-by-layer hydrogel coatings with pH-triggered hydrophobicity. *Biomaterials* **2015**, *45*, 64–71. [[CrossRef](#)]
176. George, L.; Bavva, M.C.; Rohan, K.V.; Srivastava, R. A therapeutic polyelectrolyte-vitamin C nanoparticulate system in polyvinyl alcohol-alginate hydrogel: An approach to treat skin and soft tissue infections caused by *Staphylococcus aureus*. *Colloids Surf. B Biointerfaces* **2017**, *160*, 315–324. [[CrossRef](#)]
177. Liu, K.; Dai, L.; Li, C. A lignocellulose-based nanocomposite hydrogel with pH-sensitive and potent antibacterial activity for wound healing. *Int. J. Biol. Macromol.* **2021**, *191*, 1249–1254. [[CrossRef](#)]
178. Hu, C.; Long, L.; Cao, J.; Zhang, S.; Wang, Y. Dual-crosslinked mussel-inspired smart hydrogels with enhanced antibacterial and angiogenic properties for chronic infected diabetic wound treatment via pH-responsive quick cargo release. *Chem. Eng. J.* **2021**, *411*, 128564. [[CrossRef](#)]

179. Villanueva, M.E.; Cuestas, M.L.; Perez, C.J.; Campo Dall Orto, V.; Copello, G.J. Smart release of antimicrobial ZnO nanoplates from a pH-responsive keratin hydrogel. *J. Colloid Interface Sci.* **2019**, *536*, 372–380. [[CrossRef](#)]
180. Hu, C.; Zhang, F.J.; Long, L.Y.; Kong, Q.S.; Luo, R.F.; Wang, Y.B. Dual-responsive injectable hydrogels encapsulating drug-loaded micelles for on-demand antimicrobial activity and accelerated wound healing. *J. Control. Release* **2020**, *324*, 204–217. [[CrossRef](#)]
181. Munoz-Gonzalez, P.U.; Rooney, P.; Mohd Isa, I.L.; Pandit, A.; Delgado, J.; Flores-Moreno, M.; Castellano, L.E.; Mendoza-Novelo, B. Development and characterization of an immunomodulatory and injectable system composed of collagen modified with trifunctional oligourethanes and silica. *Biomater. Sci.* **2019**, *7*, 4547–4557. [[CrossRef](#)] [[PubMed](#)]
182. Wu, M.; Chen, J.; Huang, W.; Yan, B.; Peng, Q.; Liu, J.; Chen, L.; Zeng, H. Injectable and Self-Healing Nanocomposite Hydrogels with Ultrasensitive pH-Responsiveness and Tunable Mechanical Properties: Implications for Controlled Drug Delivery. *Biomacromolecules* **2020**, *21*, 2409–2420. [[CrossRef](#)] [[PubMed](#)]
183. Liu, X.; Dou, G.; Li, Z.; Wang, X.; Jin, R.; Liu, Y.; Kuang, H.; Huang, X.; Yang, X.; Yang, X.; et al. Hybrid Biomaterial Initiates Refractory Wound Healing via Inducing Transiently Heightened Inflammatory Responses. *Adv. Sci.* **2022**, *9*, e2105650. [[CrossRef](#)] [[PubMed](#)]
184. Mayer, C.R.; Cabuil, V.; Lalot, T.; Thouvenot, R. Magnetic nanoparticles trapped in pH 7 hydrogels as a tool to characterize the properties of the polymeric network. *Adv. Mater.* **2000**, *12*, 417–420. [[CrossRef](#)]
185. Shi, L.; Zeng, Y.; Zhao, Y.; Yang, B.; Ossipov, D.; Tai, C.W.; Dai, J.; Xu, C. Biocompatible Injectable Magnetic Hydrogel Formed by Dynamic Coordination Network. *ACS Appl. Mater. Interfaces* **2019**, *11*, 46233–46240. [[CrossRef](#)]
186. Kozissnik, B.; Bohorquez, A.C.; Dobson, J.; Rinaldi, C. Magnetic fluid hyperthermia: Advances, challenges, and opportunity. *Int. J. Hyperthermia* **2013**, *29*, 706–714. [[CrossRef](#)]
187. Patwa, R.; Soundararajan, N.; Mulchandani, N.; Bhasney, S.M.; Shah, M.; Kumar, S.; Kumar, A.; Katiyar, V. Silk nano-discs: A natural material for cancer therapy. *Biopolymers* **2018**, *109*, e23231. [[CrossRef](#)]
188. Wang, Z.J.; Zhai, X.Y.; Fan, M.; Tan, H.P.; Chen, Y. Thermal-reversible and self-healing hydrogel containing magnetic microspheres derived from natural polysaccharides for drug delivery. *Eur. Polym. J.* **2021**, *157*, 110644. [[CrossRef](#)]
189. Forouzandehdel, S.; Forouzandehdel, S.; Rezaghi Rami, M. Synthesis of a novel magnetic starch-alginic acid-based biomaterial for drug delivery. *Carbohydr. Res.* **2020**, *487*, 107889. [[CrossRef](#)]
190. Nezami, S.; Sadeghi, M.; Mohajerani, H. A novel pH-sensitive and magnetic starch-based nanocomposite hydrogel as a controlled drug delivery system for wound healing. *Polym. Degrad. Stabil.* **2020**, *179*, 109255. [[CrossRef](#)]
191. Noh, M.; Choi, Y.H.; An, Y.H.; Tahk, D.; Cho, S.; Yoon, J.W.; Jeon, N.L.; Park, T.H.; Kim, J.; Hwang, N.S. Magnetic Nanoparticle-Embedded Hydrogel Sheet with a Groove Pattern for Wound Healing Application. *ACS Biomater. Sci. Eng.* **2019**, *5*, 3909–3921. [[CrossRef](#)] [[PubMed](#)]
192. Ma, W.; Dong, W.; Zhao, S.; Du, T.; Wang, Y.; Yao, J.; Liu, Z.; Sun, D.; Zhang, M. An injectable adhesive antibacterial hydrogel wound dressing for infected skin wounds. *Biomater. Adv.* **2022**, *134*, 112584. [[CrossRef](#)] [[PubMed](#)]
193. Han, K.; Bai, Q.; Wu, W.; Sun, N.; Cui, N.; Lu, T. Gelatin-based adhesive hydrogel with self-healing, hemostasis, and electrical conductivity. *Int. J. Biol. Macromol.* **2021**, *183*, 2142–2151. [[CrossRef](#)]
194. Zu, Y.; Wang, Y.; Yao, H.; Yan, L.; Yin, W.; Gu, Z. A Copper Peroxide Fenton Nanoagent-Hydrogel as an In Situ pH-Responsive Wound Dressing for Effectively Trapping and Eliminating Bacteria. *ACS Appl. Bio Mater.* **2022**, *5*, 1779–1793. [[CrossRef](#)] [[PubMed](#)]
195. Cherng, J.H.; Lin, C.J.; Liu, C.C.; Yeh, J.Z.; Fan, G.Y.; Tsai, H.D.; Chung, C.F.; Hsu, S.D. Hemostasis and Anti-Inflammatory Abilities of AuNPs-Coated Chitosan Dressing for Burn Wounds. *J. Pers. Med.* **2022**, *12*, 1089. [[CrossRef](#)]
196. Zhao, X.; Guo, B.; Wu, H.; Liang, Y.; Ma, P.X. Injectable antibacterial conductive nanocomposite cryogels with rapid shape recovery for noncompressible hemorrhage and wound healing. *Nat. Commun.* **2018**, *9*, 2784. [[CrossRef](#)] [[PubMed](#)]
197. Muthiah Pillai, N.S.; Eswar, K.; Amirthalingam, S.; Mony, U.; Kerala Varma, P.; Jayakumar, R. Injectable Nano Whitlockite Incorporated Chitosan Hydrogel for Effective Hemostasis. *ACS Appl. Bio Mater.* **2019**, *2*, 865–873. [[CrossRef](#)] [[PubMed](#)]
198. Preethi, G.U.; Unnikrishnan, B.S.; Sreekutty, J.; Archana, M.G.; Anupama, M.S.; Shiji, R.; Raveendran Pillai, K.; Joseph, M.M.; Syama, H.P.; Sreelekha, T.T. Semi-interpenetrating nanosilver doped polysaccharide hydrogel scaffolds for cutaneous wound healing. *Int. J. Biol. Macromol.* **2020**, *142*, 712–723. [[CrossRef](#)]
199. Zhao, Y.; Li, Z.; Song, S.; Yang, K.; Liu, H.; Yang, Z.; Wang, J.; Yang, B.; Lin, Q. Skin-Inspired Antibacterial Conductive Hydrogels for Epidermal Sensors and Diabetic Foot Wound Dressings. *Adv. Funct. Mater.* **2019**, *29*, 1901474. [[CrossRef](#)]
200. Yang, E.; Hou, W.; Liu, K.; Yang, H.; Wei, W.; Kang, H.; Dai, H. A multifunctional chitosan hydrogel dressing for liver hemostasis and infected wound healing. *Carbohydr. Polym.* **2022**, *291*, 119631. [[CrossRef](#)]
201. Jayaramudu, T.; Varaprasad, K.; Reddy, K.K.; Pyarasani, R.D.; Akbari-Fakhrabadi, A.; Amalraj, J. Chitosan-pluronic based Cu nanocomposite hydrogels for prototype antimicrobial applications. *Int. J. Biol. Macromol.* **2020**, *143*, 825–832. [[CrossRef](#)] [[PubMed](#)]
202. Venkataprasanna, K.S.; Prakash, J.; Vignesh, S.; Bharath, G.; Venkatesan, M.; Banat, F.; Sahabudeen, S.; Ramachandran, S.; Devanand Venkatasubbu, G. Fabrication of Chitosan/PVA/GO/CuO patch for potential wound healing application. *Int. J. Biol. Macromol.* **2020**, *143*, 744–762. [[CrossRef](#)] [[PubMed](#)]
203. Pham, T.N.; Su, C.F.; Huang, C.C.; Jan, J.S. Biomimetic hydrogels based on L-Dopa conjugated gelatin as pH-responsive drug carriers and antimicrobial agents. *Colloids Surf. B Biointerfaces* **2020**, *196*, 111316. [[CrossRef](#)] [[PubMed](#)]

204. Ali, A.; Bano, S.; Poojary, S.S.; Priyadarshi, R.; Choudhary, A.; Kumar, D.; Negi, Y.S. Comparative analysis of TiO<sub>2</sub> and Ag nanoparticles on xylan/chitosan conjugate matrix for wound healing application. *Int. J. Polym. Mater. Polym. Biomater.* **2020**, *71*, 376–385. [[CrossRef](#)]
205. Cheng, H.; Shi, Z.; Yue, K.; Huang, X.; Xu, Y.; Gao, C.; Yao, Z.; Zhang, Y.S.; Wang, J. Sprayable hydrogel dressing accelerates wound healing with combined reactive oxygen species-scavenging and antibacterial abilities. *Acta Biomater.* **2021**, *124*, 219–232. [[CrossRef](#)] [[PubMed](#)]
206. Dong, Q.; Zu, D.; Kong, L.; Chen, S.; Yao, J.; Lin, J.; Lu, L.; Wu, B.; Fang, B. Construction of antibacterial nano-silver embedded bioactive hydrogel to repair infectious skin defects. *Biomater. Res.* **2022**, *26*, 36. [[CrossRef](#)]
207. Xu, M.; Li, Q.; Fang, Z.; Jin, M.; Zeng, Q.; Huang, G.; Jia, Y.G.; Wang, L.; Chen, Y. Conductive and antimicrobial macroporous nanocomposite hydrogels generated from air-in-water Pickering emulsions for neural stem cell differentiation and skin wound healing. *Biomater. Sci.* **2020**, *8*, 6957–6968. [[CrossRef](#)]
208. Jia, Z.; Lv, X.; Hou, Y.; Wang, K.; Ren, F.; Xu, D.; Wang, Q.; Fan, K.; Xie, C.; Lu, X. Mussel-inspired nanozyme catalyzed conductive and self-setting hydrogel for adhesive and antibacterial bioelectronics. *Bioact. Mater.* **2021**, *6*, 2676–2687. [[CrossRef](#)]
209. Zhu, S.; Yu, C.; Zhao, M.; Liu, N.; Chen, Z.; Liu, J.; Li, G.; Deng, Y.; Sai, X.; Huang, H.; et al. Histatin-1 loaded multifunctional, adhesive and conductive biomolecular hydrogel to treat diabetic wound. *Int. J. Biol. Macromol.* **2022**, *209*, 1020–1031. [[CrossRef](#)]
210. Zheng, H.; Wang, S.; Cheng, F.; He, X.; Liu, Z.; Wang, W.; Zhou, L.; Zhang, Q. Bioactive anti-inflammatory, antibacterial, conductive multifunctional scaffold based on MXene@CeO<sub>2</sub> nanocomposites for infection-impaired skin multimodal therapy. *Chem. Eng. J.* **2021**, *424*, 130148. [[CrossRef](#)]
211. Liang, Y.; Wang, M.; Zhang, Z.; Ren, G.; Liu, Y.; Wu, S.; Shen, J. Facile synthesis of ZnO QDs@GO-CS hydrogel for synergetic antibacterial applications and enhanced wound healing. *Chem. Eng. J.* **2019**, *378*, 122043. [[CrossRef](#)]
212. Wang, M.; Xia, A.; Wu, S.; Shen, J. Facile Synthesis of the Cu, N-CDs@GO-CS Hydrogel with Enhanced Antibacterial Activity for Effective Treatment of Wound Infection. *Langmuir* **2021**, *37*, 7928–7935. [[CrossRef](#)] [[PubMed](#)]
213. Wang, X.; Zhou, X.; Yang, K.; Li, Q.; Wan, R.; Hu, G.; Ye, J.; Zhang, Y.; He, J.; Gu, H.; et al. Peroxidase- and UV-triggered oxidase mimetic activities of the UiO-66-NH<sub>2</sub>/chitosan composite membrane for antibacterial properties. *Biomater. Sci.* **2021**, *9*, 2647–2657. [[CrossRef](#)] [[PubMed](#)]
214. Xie, Y.Y.; Zhang, Y.W.; Liu, X.Z.; Ma, X.F.; Qin, X.T.; Jia, S.R.; Zhong, C. Aggregation-induced emission-active amino acid/berberine hydrogels with enhanced photodynamic antibacterial and anti-biofilm activity. *Chem. Eng. J.* **2021**, *413*, 127542. [[CrossRef](#)]
215. Huang, S.; Xu, S.; Hu, Y.; Zhao, X.; Chang, L.; Chen, Z.; Mei, X. Preparation of NIR-responsive, ROS-generating and antibacterial black phosphorus quantum dots for promoting the MRSA-infected wound healing in diabetic rats. *Acta Biomater.* **2022**, *137*, 199–217. [[CrossRef](#)]
216. Lu, H.; Liu, J.; Yu, M.; Li, P.; Huang, R.; Wu, W.; Hu, Z.; Xiao, Y.; Jiang, F.; Xing, X. Photothermal-enhanced antibacterial and antioxidant hydrogel dressings based on catechol-modified chitosan-derived carbonized polymer dots for effective treatment of wound infections. *Biomater. Sci.* **2022**, *10*, 2692–2705. [[CrossRef](#)]
217. Yu, R.; Li, M.; Li, Z.L.; Pan, G.Y.; Liang, Y.Q.; Guo, B.L. Supramolecular Thermo-Contracting Adhesive Hydrogel with Self-Removability Simultaneously Enhancing Noninvasive Wound Closure and MRSA-Infected Wound Healing. *Adv. Healthc. Mater.* **2022**, *11*, 2102749. [[CrossRef](#)]
218. Li, Z.; Liu, P.; Ji, X.; Gong, J.; Hu, Y.; Wu, W.; Wang, X.; Peng, H.Q.; Kwok, R.T.K.; Lam, J.W.Y.; et al. Bioinspired Simultaneous Changes in Fluorescence Color, Brightness, and Shape of Hydrogels Enabled by AIEgens. *Adv. Mater.* **2020**, *32*, e1906493. [[CrossRef](#)]
219. Hoare, T.; Santamaria, J.; Goya, G.F.; Irusta, S.; Lin, D.; Lau, S.; Padera, R.; Langer, R.; Kohane, D.S. A Magnetically Triggered Composite Membrane for On-Demand Drug Delivery. *Nano Lett.* **2009**, *9*, 3651–3657. [[CrossRef](#)]
220. Caldorera-Moore, M.E.; Liechty, W.B.; Peppas, N.A. Responsive Theranostic Systems: Integration of Diagnostic Imaging Agents and Responsive Controlled Release Drug Delivery Carriers. *Acc. Chem. Res.* **2011**, *44*, 1061–1070. [[CrossRef](#)]
221. Wu, B.Y.; Le, X.X.; Jian, Y.K.; Lu, W.; Yang, Z.Y.; Zheng, Z.K.; Theato, P.; Zhang, J.W.; Zhang, A.; Chen, T. pH and Thermo Dual-Responsive Fluorescent Hydrogel Actuator. *Macromol. Rapid Commun.* **2019**, *40*, e1800648. [[CrossRef](#)] [[PubMed](#)]
222. Sabbagh, F.; Kim, B.S. Recent advances in polymeric transdermal drug delivery systems. *J. Control. Release* **2022**, *341*, 132–146. [[CrossRef](#)] [[PubMed](#)]
223. Bergert, M.; Lembo, S.; Sharma, S.; Russo, L.; Milovanovic, D.; Gretarsson, K.H.; Bormel, M.; Neveu, P.A.; Hackett, J.A.; Petsalaki, E.; et al. Cell Surface Mechanics Gate Embryonic Stem Cell Differentiation. *Cell Stem Cell* **2021**, *28*, 209–216.e4. [[CrossRef](#)] [[PubMed](#)]
224. Bongiorno, T.; Kazlow, J.; Mezencev, R.; Griffiths, S.; Olivares-Navarrete, R.; McDonald, J.F.; Schwartz, Z.; Boyan, B.D.; McDevitt, T.C.; Sulchek, T. Mechanical stiffness as an improved single-cell indicator of osteoblastic human mesenchymal stem cell differentiation. *J. Biomech.* **2014**, *47*, 2197–2204. [[CrossRef](#)]

225. Lima, J.; Goncalves, A.I.; Rodrigues, M.T.; Reis, R.L.; Gomes, M.E. The effect of magnetic stimulation on the osteogenic and chondrogenic differentiation of human stem cells derived from the adipose tissue (hASCs). *J. Magn. Magn. Mater.* **2015**, *393*, 526–536. [[CrossRef](#)]
226. Mareziak, M.; Smieszek, A.; Tomaszewski, K.A.; Lewandowski, D.; Marycz, K. The effect of low static magnetic field on osteogenic and adipogenic differentiation potential of human adipose stromal/stem cells. *J. Magn. Magn. Mater.* **2016**, *398*, 235–245. [[CrossRef](#)]

**Disclaimer/Publisher’s Note:** The statements, opinions and data contained in all publications are solely those of the individual author(s) and contributor(s) and not of MDPI and/or the editor(s). MDPI and/or the editor(s) disclaim responsibility for any injury to people or property resulting from any ideas, methods, instructions or products referred to in the content.